Identification of microRNAs that stabilize p53 in HPV-positive cancer cells

Gustavo Martínez-Noël [a], Patricia Szajner [a], Rebecca E. Kramer [a], Kathleen A. Boyland [a], Asma Sheikh [a], Jennifer A. Smith [a,b], and Peter M. Howley [a#]

[a]Department of Immunology, Harvard Medical School, 77 Avenue Louis Pasteur, Boston MA 02115

[b]ICCB-Longwood Screening Facility, Harvard Medical School, 250 Longwood Avenue, Boston MA 02115

Running Title: HPV p53 miRNA Stabilization Screen

Abstract word count: 250

Text word count: 6030

#Corresponding author: Peter M. Howley, peter_howley@hms.harvard.edu

Gustavo Martínez-Noël and Patricia Szajner contributed equally to this work.

Abstract

Etiologically, 5% of all cancers worldwide are caused by the high-risk human papillomaviruses (hrHPVs). These viruses encode two oncoproteins (E6 and E7) whose expression is required for cancer initiation and maintenance. Among their cellular targets are the p53 and the retinoblastoma tumor suppressor proteins. Inhibition of the hrHPV E6-mediated ubiquitylation of p53 through the E6AP ubiquitin ligase results in the stabilization of p53, leading to cellular apoptosis. We utilized a live cell high throughput screen to determine whether exogenous microRNA (miRNA) transfection had the ability to stabilize p53 in hrHPV-positive cervical cancer cells expressing a p53-fluorescent protein as an *in vivo* reporter of p53 stability. Among the miRNAs whose transfection resulted in the greatest p53 stabilization was 375-3p that has previously been reported to stabilize p53 in HeLa cells, providing validation of the screen. The top 32 miRNAs in addition to 375-3p were further assessed using a second cell-based p53 stability reporter system as well as in non-reporter HeLa cells to examine their effects on endogenous p53 protein levels, resulting in the identification of 23 miRNAs whose transfection increased p53 levels in HeLa cells. While a few miRNAs that stabilized p53 led to decreases in E6AP protein levels, all targeted HPV oncoprotein expression. We further examined subsets of these miRNAs for their abilities to induce apoptosis and determined whether it was p53-mediated. The introduction of specific miRNAs revealed surprisingly heterogeneous responses in different cell lines. Nonetheless, some of the miRNAs described here have potential as therapeutics for treating HPV-positive cancers.

43 # Importance

44 Human papillomaviruses cause approximately 5% of all cancers worldwide and
45 encode genes that contribute to both the initiation and maintenance of these cancers. The
46 viral oncoprotein E6 is expressed in all HPV-positive cancers and functions by targeting the
47 degradation of p53 through the engagement of the cellular ubiquitin ligase E6AP. Inhibiting
48 the degradation of p53 leads to apoptosis in HPV-positive cancer cells. Using a high
49 throughput live cell assay we identified several miRNAs whose transfection stabilize p53 in
50 HPV-positive cells. These miRNAs have the potential to be used in the treatment of HPV-
51 positive cancers.

52 # Introduction

53 Cervical cancer is the second leading cause of cancer deaths among women
54 worldwide, with approximately 500,000 new cases diagnosed and 275,000 deaths each
55 year. Virtually all cases of cervical cancer are attributable to infection by HPVs. There are
56 over 200 different HPV types and a subset of these are linked to anogenital tract infections,
57 14 of which are referred to as hrHPV because they are associated with lesions that can
58 progress to cancer (1). These same hrHPVs are also associated with other genital tract
59 cancers (penile, vaginal, vulvar, and anal), as well as an increasing number of
60 oropharyngeal cancers. Indeed, approximately 5% of all cancers worldwide are caused by
61 hrHPVs (2).

62 Despite the success of the virus like particle (VLP)-based vaccine that has the
63 potential to prevent millions of new HPV-associated cancers, there is the need for effective
64 therapies to treat cancers that will develop in individuals who have not been vaccinated

65 and those already infected with hrHPVs. In this regard, hrHPVs provide a number of
66 potential viral targets for specific HPV antiviral therapies, including the viral encoded
67 oncoproteins E6 and E7, the viral E1 helicase, and the viral E2 regulatory protein.

68 The hrHPVs associated with cervical cancer encode two oncoproteins, E6 and E7,
69 that are invariably expressed in HPV-positive cancers and target the important cellular
70 growth regulatory proteins p53 and pRb, respectively (1). These cancers are dependent on
71 the continued expression of E6 and E7 and silencing these oncoproteins results in
72 apoptosis and senescence (3, 4). The E6 proteins of the hrHPV types promote the ubiquitin-
73 dependent degradation of the p53 protein (5) through its binding to the E3 ubiquitin ligase
74 E6AP (also known as UBE3A), which ubiquitylates p53 (6-8). In promoting the ubiquitin-
75 dependent proteolysis of p53, E6 counters E7-mediated replication stress signals that
76 activate and stabilize p53 (9). Thus, inhibition of the E6/E6AP-mediated ubiquitylation of
77 p53 is pro-apoptotic and provides a validated target for HPV-positive cancers. For example,
78 direct targeting of E6 induces apoptosis in HPV-positive cancer cells (10). Although the
79 hrHPV E6 proteins have other cellular activities that have been described in the literature,
80 we have focused on the E6/E6AP pathway as a potential therapeutic target for HPV-
81 positive cancers, as well as precancerous lesions.

82 MicroRNAs (miRNAs/miRs) are small non-coding RNAs (approximately 22
83 nucleotides in length) that significantly impact and regulate many essential biological
84 pathways. miRNAs negatively regulate gene expression either by translational repression
85 or cleavage of target mRNAs. Many miRNAs have been shown to play roles in cancer,
86 sometimes as oncogenes and other times as tumor suppressors, making them suitable as
87 therapeutic targets. miRNAs themselves can be used as cancer therapeutics as they may

88 affect one or more pathways essential for the replication and survival of specific cancer
89 cells. There have been a number of studies focused on HPV and miRNAs in recent years.
90 These studies have examined whether HPVs, like many other viruses, encode viral miRNAs
91 (11) and whether the HPV oncoproteins regulate the expression of cellular miRNAs (12).
92 Other studies have proposed miRNAs as potential biomarkers of hrHPV infections (13).
93 There have also been studies that examined the effects of miRNA expression in various
94 cancers including cervical cancers (For review see (14)). It was with this mindset that we
95 conducted a screen to identify miRNAs whose transfection into HPV-positive cancer cells
96 stabilize p53.

97 Here we present a high throughput screen using a cell-based platform to assay p53
98 stability in hrHPV E6-expressing HeLa cells that identified miRNAs whose transfection
99 increased p53 protein levels. Several of these miRNAs caused apoptosis and/or p21
100 induction when transfected into hrHPV-positive cells. The goal of this work was to find
101 miRNAs that could be used as therapeutic tools for the treatment of hrHPV-associated
102 diseases, regardless of whether these miRNAs are physiological regulators of p53 stability.
103 To our knowledge, this is the first study to systematically exam miRNAs for their abilities to
104 stabilize p53 in hrHPV-positive cancer cells. We also provide insights into the mechanisms
105 by which some of these miRNAs function in stabilizing p53 and promoting apoptosis.

106 Results

107 A high throughput screen identified transfected miRNAs that
108 stabilize p53 in HeLa cells.

109 To identify miRNAs that stabilize p53 and induce apoptosis when transfected into
110 hrHPV-positive cancer cells, we performed a high throughput screen in HPV18-positive
111 HeLa cells harboring a reporter for p53 protein stability. The reporter was originally
112 designed by the Elledge lab for their "global protein stability system"(15, 16), and
113 expresses a bicistronic mRNA that encodes an EGFP-p53 fusion protein and the red
114 fluorescent protein DsRed as reference (Figure 1A). The stability of the EGFP-p53 fusion
115 protein is determined by the less stable protein, in this case p53, with a half-life less than
116 30 minutes in HeLa cells due to E6/E6AP-mediated proteolysis (5, 17). To detect changes
117 in p53 stability, we monitored the EGFP/DsRed fluorescence ratio by laser scanning
118 cytometry. In our screen, for the fusion protein we used a p53 gene encoding the R273C
119 mutant, which is also efficiently targeted by E6/E6AP for ubiquitin-dependent proteolysis
120 (18). Because this mutant is defective in DNA binding (19, 20) and probably in the p53
121 mitochondrial pro-apoptotic pathways (21), it does not add an extra pro-apoptotic
122 stimulus to the eventual stabilization of the endogenous p53 during the course of the assay.
123 Furthermore, p53(R273C) can interfere with p53 transcriptionally driven apoptosis (22),
124 thus facilitating the acquisition of data for p53 stabilizers that might otherwise kill all cells.
125 The results of this screen, which assayed 885 miRNA mimics, are shown in Figure 1B and
126 Table S1. The top hit, 375-3p, has been previously reported to stabilize p53 in HPV-positive
127 cells (23) providing validation for this screen. Of note, since all the miRNAs used in this
128 study are human, we omitted the use of the prefix hsa-miR in the miRNAs names. We
129 selected for further testing the miRNAs that produced the next 32 highest EGFP/DsRed
130 fluorescence ratios (Table 1).

131 To confirm the results obtained in the screen, we tested the selected miRNAs in
132 HeLa cells containing a different bicistronic reporter vector that has been successfully used
133 in a small molecule screen to find p53 stabilizers in HeLa cells (24). In this vector,
134 p53(R273C) is fused to mRuby, a bright monomeric red fluorescent protein, and the
135 reference monomeric green fluorescent protein SGFP2 is fused to H2B (Figure 2A). For this
136 experiment, we determined the percentage of H2B-SGFP2 expressing cells that also
137 expressed mRuby-p53 (R273C) using flow cytometry. Two randomly selected miRNAs
138 (498-5p and 665), which were negative in the initial screen, and the miRNA Ctrl. 1 were
139 used as negative controls, along with 375-3p used as a positive control. As shown in Figure
140 2B, 25 of the 32 originally selected miRNAs were confirmed as significantly stabilizing
141 mRuby-p53 (R273C) in this reporter HeLa cell line.

142 Validation of candidate miRNAs in HeLa cells

143 Twenty seven miRNAs were next tested for their ability to stabilize endogenous p53
144 in HeLa cells by western blotting (Figure 3 and Table S2), including 3 miRNAs, 17-5p, 153-
145 3p, and 592 that produced a moderate increase in the levels of the reporter p53 . While
146 transfection of most of the miRNAs resulted in some degree of p53 stabilization compared
147 to the mock and negative controls, four miRNAs (219-5p, 106a-3p, 592, and 508-3p) had
148 little or no effect on endogenous p53 levels. The other miRNAs ranged from those that
149 produced a mild to moderate increase in p53 levels (511-5p, 519d-3p, 631, 374a-3p, 153-
150 3p, 17-5p, 373-3p, 210-3p, and 302c-3p) to those that caused stronger p53 stabilization
151 (519c-3p, 943, 374b-5p, 148b-5p, 519b-3p, 93-3p, 520d-3p, 520c-3p, 520b-3p, 519a-3p,
152 302a-3p, 302b-3p, 509-3p, and 1287-5p). We also examined the effects of the miRNAs on
153 E6AP and HPV18 E6 protein levels (Figure 4A-F and Table S2). Although most miRNAs had

154 little or no effect on E6AP levels, miRNAs 148b-5p, 374a-3p, and 374b-5p decreased the
155 levels of E6AP to values comparable to those observed in cells transfected with the positive
156 control 375-3p, which has been previously shown to target the E6AP mRNA (23).
157 Transfection of a few miRNAs, most notably 93-3p and 1287-5p, resulted in elevated levels
158 of E6AP. In contrast, transfection of most of the miRNAs tested in this experiment led to a
159 reduction in E6 protein levels. While there was no correlation between the protein levels of
160 E6 and E6AP ($r(35) = 0.02098$, $p = 0.9019$) or between E6AP and p53 ($r(35) = -0.07389$, p
161 $= 0.6638$), there was a significant negative correlation between the levels of E6 and p53
162 ($r(35) = -0.6288$, $p<0.0001$) (Figure 4G), suggesting that a decrease in E6 expression plays
163 a significant role in the stabilization of p53 by several of these miRNAs in HeLa cells.
164 Examination of these data suggest that, under the conditions used in this experiment, a
165 ~50% reduction in E6 protein levels appears necessary for p53 stabilization in HeLa cells.
166 Sequence analysis of the validated miRNAs showed a significant enrichment of miRNAs
167 sharing a common seed sequence (5'-AAGUGC-3') that defines the 302-3p/372-3p/373-
168 3p/519-3p/520-3p family of miRNAs (from now on referred as 302/519 miRNA family)
169 (Figure 5). Based on these results, we selected miRNAs 148b, 374a, 374b, 1287, and five
170 members of the 302/519 family for further analysis.

171 Transfection of selected miRNAs increase p53 in different
172 hrHPV-positive cell lines.

173 To examine whether there was any HPV specificity to the stabilization of p53 by
174 these miRNAs, we examined their effects on the stability of p53 in other hrHPV-positive
175 cancer cell lines. We transfected three cervical cancer cell lines, SiHa (HPV16), ME-180

176 (HPV68), and MS751 (HPV45), as well as two head and neck squamous carcinoma cell
177 lines, UM-SCC-47 and UM-SCC-104 (both HPV16), with the selected miRNAs and examined
178 p53, E6AP, and actin protein levels by western blot. As shown in Figure 6A-E, the
179 transfection of these miRNAs increased the protein levels of p53 in all HPV-positive cell
180 lines, indicating this effect is conserved in other HPV-associated cervical cancer cell lines
181 independent of the hrHPV type. However, the relative magnitude of the p53 stabilization by
182 individual miRNAs varied in the five HPV-positive cell lines, likely reflecting differences
183 between the cell lines and/or HPV types. 519d-3p consistently produced the lowest
184 increase in p53 protein levels compared to the other 302/519 miRNA family members
185 used in these experiments. These miRNAs share considerable sequence homology
186 throughout and the same seed sequence with exception of 519d-3p, whose seed sequence
187 is displaced one position by the addition of a C at its 5' end (Figure 5). This suggests that a
188 good pairing of the seed sequence of these miRNAs with their target mRNA is important for
189 the ability of the members of 302/519 miRNA family to induce accumulation of p53 when
190 transfected into hrHPV-positive cancer cells.
191 To evaluate the involvement of the E6/E6AP pathway in the stabilization of p53 by
192 these miRNAs, we examined their effects on the levels of p53 and E6AP in HPV-negative
193 human U2OS cells (Figure 6F), an osteosarcoma-derived cell line that harbors wt p53
194 under the control of Mdm2. Transfection of miRNAs 375-3p and 148b-5p increased the
195 levels of p53 in U2OS cells, indicating that these two miRNAs can affect p53 protein levels
196 independent of HPV oncoprotein expression. In contrast, transfection of the miRNAs from
197 the 302/519 family and 1287-5p had minimal or no effect on the levels of p53 in U2OS
198 cells, suggesting that the effect of these miRNAs on p53 stability is dependent upon the

199 expression of hrHPV E6. Of note, transfection of miRNAs 375-3p, 148b-5p and to a lesser
200 degree 374a-3p and 374b-5p, decreased the levels of E6AP in each of the cell lines
201 analyzed.

202 Several miRNAs decrease expression of E6/E7.

203 Since the increase of p53 in HeLa cells transfected with the miRNAs identified in this
204 study negatively correlated to the levels of E6 (Figure 4G), we hypothesized that the ability
205 of these miRNAs to stabilize p53 in HPV-positive cancer cells might be mediated, at least in
206 part, by a negative effect on E6 expression. This could be a consequence of destabilizing the
207 E6 protein or decreasing its expression, either by targeting the E6/E7 mRNAs for
208 degradation, preventing their translation, or decreasing viral transcription. We observed
209 that transfection of these miRNAs into HeLa cells, particularly members of the 302/519
210 family and 1287-5p, decreased both E6 and E7 protein levels similarly (Figure 7A). This is
211 consistent with the idea that these miRNAs affect the expression of the viral E6/E7 mRNAs
212 since the hrHPV E6 and E7 genes are expressed from a single promoter located in the viral
213 LCR. This effect on the level of the E6/E7 mRNA in HeLa cells was confirmed by qRT-PCR
214 using primers that detect all HPV E6/E7 transcripts (Figure 7B). Interestingly, all miRNAs
215 tested, including 375-3p and 148b-5p that increased p53 protein levels in the absence of
216 hrHPV proteins (Figure 6F), also decreased the levels of the E6/E7 transcripts. Although
217 498-5p reduced the level of the E6/E7 mRNAs in HeLa cells, consistent with the reduced
218 level of E6 protein shown in Figures 3, 4 and 7A, we did not observe an increase in p53
219 protein levels (Figures 3 and 6). While 375-3p was as efficient in repressing the expression
220 of the E6/E7 mRNAs in HPV16 SiHa cells as in HPV18 HeLa cells, most of the tested
221 miRNAs were less efficient decreasing the levels of the E6/E7 transcripts in SiHa cells, even

222 though they were efficiently transfected as determined by siGlo RISC-free transfection
223 control (data not shown). In addition to 375-3p, only 519b-3p and 1287-5p showed
224 comparable effects on the E6/E7 transcripts in both HPV-positive cell lines. Surprisingly,
225 148b-5p, which stabilized p53 in SiHa cells, produced an increase in the levels of the E6/E7
226 mRNAs but we could not confirm whether E6 protein levels were affected in this cell line
227 (e.g. by preventing translation) because we were unable to detect HPV16 E6 using any of
228 the commercially available anti-HPV16 E6 antibodies.

229 To determine whether these miRNAs were targeting the untranslated regions (UTR)
230 of the HPV16 E6/E7 mRNAs, we examined their effect in 1321 cells, a human keratinocyte
231 cell line that expresses HPV16 E6/E7 under the control of the human β-actin promoter and
232 from a mRNA containing the 3'UTR of the human β-actin mRNA (25). In this cell line, the
233 302/519 miRNA family members (302a-3p, 373-3p, 519b-3p, 519d-3p, and 520c-3p) and
234 1287-5p failed to increase the p53 protein levels, suggesting that their effect involves
235 actions over the promoter activity of the HPV16 LCR and/or the 3'UTR of the E6/E7
236 transcripts (Figure 7C). In contrast, 375-3p, 148b-5p, 374a-3p, and 374b-5p transfection
237 resulted in an increase in p53 protein levels, indicating it is likely through a different
238 mechanism than the miRNAs of the 302/519 family and 1287-5p. Considering that the
239 E6/E7 transcripts in the different hrHPV-positive cell lines tested have different 3'UTRs,
240 depending on the viral sequence inserted in the host cell and the insertion site, it is more
241 likely that the miRNAs of the 302/519 family and 1287-5p affect E6 and E7 protein levels
242 by acting on the viral LCR promoter activity. In line with this hypothesis, 1287-5p and the
243 302/519 family members efficiently repressed the HPV16 LCR and HPV18 LCR promoter
244 activity in a reporter system in the HPV-negative cervical cancer cells C33A (Figure 7D),

245 **Selected miRNAs induce apoptosis and/or p21 expression.**

246 Stabilization of p53 is expected to be pro-apoptotic in hrHPV-positive cells. We
247 therefore tested whether miRNAs that stabilized p53 in HeLa cells induce apoptosis. Flow
248 cytometric analysis of HeLa cells transfected with different miRNAs and stained with the
249 apoptosis marker Annexin V revealed an increase in the fraction of apoptotic cells when
250 compared to untreated or mock transfected cells (Figure 8A). Of note, miRNAs Ctrl.1 and
251 498-5p, which did not increase p53 levels in hrHPV-positive cells (Figures 3 and 6), did
252 increase Annexin V staining upon transfection into HeLa cells. In contrast, there was a
253 correlation between induction of apoptosis and stabilization of p53 in HeLa cells
254 transfected with the 302/519 family members (Figure 3). In this family, 519d-3p, which
255 produced the lowest increase in p53 levels in HeLa cells, was also the least efficient in
256 inducing apoptosis.

257 We next examined the ability of a subset of these miRNAs to induce apoptosis in
258 SiHa cells and two HPV-negative cancer cell lines, C33A and U2OS, using Annexin V staining
259 (Figure 8B). Transfection with the miRNA 20a-3p was utilized as a negative control, since it
260 does not induce apoptosis in cervical cancer cells (26). The 1287-5p miRNA was also
261 included in these experiments as it was found to stabilize p53 (Figures 3 and 6) and to
262 efficiently decrease E6/E7 mRNAs expression in both HeLa and SiHa cells (Figure 7B).
263 Similar to their effect in HeLa cells, 148b-5p and 1287-5p induced apoptosis in SiHa cells
264 whereas 375-3p and 519b-3p had very little or no effect. While all of these miRNAs
265 increased the levels of p53 when transfected into SiHa cells (Figure 6A), 148b-5p and
266 1287-5p led to the highest p53 levels. Both 148b-5p and 1287-5p stimulated apoptosis in
267 C33A cells, an HPV-negative cervical cancer cell line that already expresses high levels of an

268 inactive mutant form of p53 (27), indicating that these miRNAs can induce apoptosis
269 independently of p53.

270 Since 519b-3p has been reported to induce senescence in HeLa cells through p21
271 expression, which is partially dependent of p53 (28), we tested whether other members of
272 the 302/519 family have a similar effect on p21 protein levels and if it also occurs in
273 HPV16-positive SiHa cells. Since 375-3p has been shown to increase p21 protein levels in
274 both HeLa and SiHa cells (23), it was included as the positive control. As shown in Figure
275 8C, the miRNAs of the 302/519 family tested in this experiment increased p21 protein
276 levels in both cell lines with the exception of 519d-3p, which did not increase p21 levels in
277 SiHa cells. Interestingly, 498-5p led to an increase in p21 protein levels in SiHa cells;
278 however this is likely to be at least partially p53 independent since this miRNA failed to
279 induce a marked p53 accumulation under similar conditions in these cells (Figure 6A).

280 miRNAs of the 302/519 family and 1287-5p induce p53-
281 dependent apoptosis in HeLa cells.

282 We next examined if induction of apoptosis by several representative miRNAs is
283 p53-dependent in HeLa cells. We performed Annexin V staining of HeLa cells co-
284 transfected with the miRNAs and an siRNA targeting p53 or its C911 variant (29) to
285 address possible off-target effects of the siRNA (Figure 9A). As expected, the positive
286 control 375-3p increased the percentage of Annexin V-stained cells while 20a-3p had no
287 significant effect when compared to untreated cells. Surprisingly, the apoptotic effect of
288 375-3p was independent of p53 since knock-down of p53 had little effect on the percentage
289 of apoptotic cells in HeLa cells co-transfected with this miRNA. The effect of 498-5p on

290 apoptosis is also p53-independent and consistent with the inability of this miRNA to
291 stabilize p53 when transfected into hrHPV-positive cell lines (Figures 3 and 6). Similarly,
292 the apoptotic effects of miRNAs 148b-5p and 374a-3p are also independent of p53, as co-
293 transfection of these miRNAs with either the siRNA against p53 or its C911 version have
294 similar effects on the percentage of apoptotic cells. This indicates that, in these cases, the
295 effect observed when p53 is knocked down can be attributed to off-target effects of the
296 siRNA against p53. In contrast, the numbers of apoptotic cells observed with 519b-3p (as a
297 representative of the 302/519 family of miRNAs) and 1287-5p were reduced when co-
298 transfected with the p53 siRNA but not with its C911 version, suggesting that the apoptotic
299 effect of these miRNAs is largely dependent on p53 in HeLa cells. Similar results were
300 observed when using PARP cleavage as a marker for apoptosis in western blot analysis (Fig
301 9B).

302 # Discussion

303 In this study we identified several miRNAs that increased p53 protein levels when
304 transfected in HeLa cells. Some of the miRNA hits from our high throughput screen (148b-
305 5p, 302a-3p, 373-3p, and 374b-5p) have been previously reported to have decreased
306 expression in cervical cancer cells and tissues compared to the controls used in each of the
307 studies (26, 30-32). Another positive miRNA from the screen, 1287-5p, has been found to
308 have no change in its expression level in cervical cancer cells, but is sequestered away from
309 its targets by the circular RNA circSLC26A4, which is overexpressed in hrHPV-positive
310 cancer cells (33). Together these findings suggest that interfering with the functions of
311 some of the miRNAs identified in this work might contribute to the establishment of HPV

312 infections or/and progression of hrHPV-infected cells towards cancer. Consistent with that,
313 several of the miRNAs identified in our screen, namely 148b-5p, 302a-3p, 374b-5p, or
314 519b-3p, have been shown to slow cell growth and induce apoptosis in hrHPV-positive
315 cervical cancer cells (28, 31, 32, 34, 35). Taken together, these previous findings validate
316 this screening platform as a reliable tool to identify miRNAs that affect the cell growth and
317 survival of hrHPV-positive cells, as expected from miRNAs whose transfection stabilize
318 p53.

319 Since the ubiquitin ligase activity of E6AP/E6 is responsible for the efficient
320 proteolysis of p53 in hrHPV-positive cervical cancer cells, we determined whether
321 transfection of any of the miRNAs identified in this screen altered the levels of E6AP in
322 HeLa cells. Interestingly, only three of the 27 miRNAs analyzed in HeLa cells, 148b-5p,
323 374a-3p, and 374b-5p, led to a decrease in E6AP protein levels comparable to the decrease
324 produced by 375-3p. Although we did not determine whether they directly bind to the
325 E6AP mRNA, target prediction analysis using the miRDB database (www.mirdb.org) (36,
326 37) revealed that 148b-5p and 374b-5p each have three sites complementary to their seed
327 sequences within the 3'UTR of the E6AP mRNA. Remarkably, these four miRNAs (148b-5p,
328 374a-3p, 374b-5p, and 375-3p) also led to decreased E6 expression. This simultaneous
329 decrease of both E6AP and E6 may be required to stabilize p53 in HeLa cells, since a small
330 amount of E6AP is sufficient to efficiently promote p53 degradation in this cell line
331 (38). The need to suppress the very efficient E6/E6AP-mediated degradation of p53 to
332 increase the levels of this protein in hrHPV-positive cancer cells is exemplified by miRNAs
333 375-3p and 1287-5p. Both miRNAs stabilized p53 in absence of E6 when transfected into
334 U2OS cells, however, they also efficently decrease the levels of E6 when transfected into

335 HeLa and SiHa cells, suggesting that this is a necessary condition to stabilize p53 in these
336 cells. Moreover, in this study we haven't found any miRNA that stabilize p53 in hrHPV-
337 cancer cells that do not significantly decrease the E6 protein level too. In contrast,
338 transfection of 498-5p, which also resulted in decreased levels of E6 in these cells, did not
339 stabilize p53 in HeLa cells, suggesting that the remaining E6 protein was sufficient to target
340 p53 for degradation. In line with this idea, in our study, miRNAs that failed to reduce E6
341 protein levels to approximately half of its original amount or beyond also failed to increase
342 p53 levels in HeLa cells, suggesting that there is a considerable excess of E6 in these cells
343 that must be overcome to stabilize p53. High levels of expression of E6 could therefore be a
344 limiting factor for the use of some miRNAs such as 498-5p as therapeutics, at least in some
345 hrHPV-associated cancers.

346 While several of the transfected miRNAs were found to induce apoptosis, the
347 mechanisms by which this occurred varied. The apoptotic induction in HeLa cells for three
348 of the miRNAs, 148b-5p, 374a-3p, and 375-3p, was independent of p53 stabilization. In
349 contrast, transfection of 1287-5p induced apoptosis in HeLa cells in a p53-dependent
350 manner. The miRNA 1287-5p was also found to efficiently induce apoptosis in U2OS cells
351 without a noticeable increase in p53 levels and to increase the number of apoptotic C33A
352 cells, which do not express wt p53, indicating that this miRNA promotes cell death
353 independent of p53 stabilization in these HPV-negative cells. Therefore, 1287-5p can
354 induce apoptosis via different pathways depending on the cell type. This is also exemplified
355 by Ctrl. 1 whose transfection stabilized p53 only in U2OS cells. The other miRNA that we
356 found to induce apoptosis in HeLa cells in a p53-dependent manner upon transfection was
357 519b-3p, a member of the 302/519 family. Abdelmohsen and colleagues have previously

358 reported that 519-3p transfection in HeLa cells increases p21 levels in a partly p53-
359 independent manner, resulting in growth inhibition and cell survival (28). There are a
360 number of technical differences between our study and that of Abdelmohsen et al. which
361 could account for the discordant results, including different miRNA concentrations and end
362 points. However, we both found that 519b-3p transfection did not induce apoptosis in SiHa
363 cells, but led to an increase in p53 and p21 protein levels. It has been reported that p53
364 must accumulate to a threshold level to induce apoptosis (39). Thus, it is feasible that
365 under the experimental conditions used in our study 519b-3p did not increase p53 levels to
366 the threshold necessary to trigger apoptosis in SiHa cells. In addition, we observed that
367 transfection of all miRNAs belonging to the 302/519 family, with the exception of 519d-3p
368 in SiHa cells, increased p21 protein levels in hrHPV-positive cells indicating this is a family
369 characteristic rather than a feature of 519b-3p alone.

370 Throughout this study, 519d-3p has been less efficient than the other members of
371 the 302/519 family of miRNAs in promoting increased p53 and p21 protein levels in the
372 hrHPV-positive cell lines, as well as in repressing expression from the HPV16 and HPV18
373 LCRs, and inducing apoptosis in HeLa cells. In addition to a few base substitutions in the 3'
374 end sequences, a difference between 519d-3p and the other miRNAs of this family included
375 in this study is the addition of a C at its 5'end. This additional nucleotide produces a
376 displacement of the miRNA sequences, including its seed sequence, which is 5'-AAAGUG-3'
377 instead of 5'- AAGUGC-3', the most common seed sequence between the members of the
378 302/519 family. Since a seed sequence match is very important for miRNA target
379 recognition (40, 41), this change in 519d-3p's seed sequence is expected to impact its
380 functions when compared to the other members of the 302/519 family. The data presented

381 in this study supports this hypothesis and indicate that the correct matching of the seed
382 sequence 5'-AAGUGC-3' with their target mRNAs is an important factor mediating the
383 effects of this family of miRNAs on p53 and p21 protein levels as well as on cell growth and
384 survival of hrHPV-positive cancer cells.

385 Since their discovery in 1993 (42, 43), the interest in miRNAs continues to increase.
386 Research in miRNAs is being translated into diagnostics as miRNAs are considered
387 sensitive and specific biomarkers. In contrast, their use as therapeutics have lagged with
388 only a few clinical trials currently underway (reviewed in (44, 45)). This may be due in part
389 to the lack of single target specificity characteristic of miRNAs. This multiplicity of targets
390 makes miRNAs potentially challenging as therapeutics because of the possibility of
391 unexpected and/or undesirable side effects. However, this property makes them an
392 attractive tool for cancer treatment since miRNAs can simultaneously regulate multiple
393 cellular pathways by modulating the expression of several genes in a coordinated fashion.
394 The utility of miRNAs as therapeutic tools will be improved by a more complete
395 understanding of how they function in the cellular networks in which they are embedded.
396 In this study, we identified several miRNAs that stabilize p53 in hrHPV-cancer cells and
397 induce apoptosis in HeLa cells in a p53-dependent or in p53-independent manner. Despite
398 the heterogenicity of the responses to different miRNAs, decreasing E6 protein levels
399 seems to be required to increase p53 protein levels in HeLa cells since all miRNAs found to
400 stabilize p53 also affected the expression of E6. Further research into the mechanisms
401 involved in the stabilization of p53 and/or induction of apoptosis by these miRNAs in
402 hrHPV-positive cells will improve our understanding of the hrHPV-host interactions and

403 contribute to the identification of new potential therapeutic targets for hrHPV infections
404 and cancers.

405 Materials and methods

406 Plasmids

407 To create a lentiviral reporter vector to monitor the protein levels of p53 *in vivo* in
408 hrHPV cancer cells, the p53 open reading frame (ORF) carrying the mutation R273C was
409 first amplified by PCR using the primers hp53-1 (5'-CACCATGGAGGAGCCGCAGTCAGATCC-
410 3') and hp53-8 (5'-GGATCCTCAGTCTGAGTCAGGCCCTTCTGTCTTG-3') and cloned into the
411 pENTR/D-TOPO vector (ThermoFisher) generating the entry vector pENTR p53(R273C)
412 (p6140). The p53(R273C) ORF was then recombined from the entry vector into a lentiviral
413 vector containing a GPS (Global Protein Stability) cassette (gift from S. Elledge) using the
414 GATEWAY cloning system (ThermoFisher), resulting in the vector pHAGE-P CMVt N-RIG2
415 p53(R273C) (p7987). The GPS reporter cassette expresses a bicistronic mRNA encoding
416 EGFP fusion proteins and the red fluorescent protein DsRed as reference (15, 16, 46, 47).
417 The reporter vector pHAGE-N CMVt N-RIG3 p53(R273C) (p7709), which contains a variant
418 of the GPS reporter cassette, expresses p53(R273C) fused to the monomeric red
419 fluorescent protein mRuby and a monomeric green fluorescent protein (SGFP2) fused to a
420 histone 2B (H2BC11) as reference (38).

421 Cell lines

422 HeLa, HeLa RIG2 p53(R273C), HeLa RIG3 p53(R273C), Siha (ATCC® HTB-35™),
423 C33A (ATCC® HTB-31™), U2OS (ATCC® HTB-96™), ME-180 (ATCC® HTB-33™), MS-751

424 (ATCC® HTB-34™), UM-SCC-47 and UM-SCC-104 (EMD-Millipore), and human
425 keratinocytes immortalized by HPV16 E6 and E7 expressed from the β-actin promoter
426 (p1321) (25) referred to here as 1321 cells were grown in Dulbecco's modified Eagle's
427 medium (DMEM) supplemented with 10% (v/v) fetal bovine serum at 37°C 5% CO2.

428 **miRNA screen**

429 For the primary miRNA screen, HeLa RIG2 p53(R273C) cells were reverse
430 transfected with the Ambion Human Pre-miR miRNA Mimic Library (2009) based on
431 miRBase release 13.0. in a one-target, one-well format using 384-well microtiter plates in a
432 high throughput format. The Z'-factor (48) was calculated for each assay plate and was
433 consistently > 0.6, indicating assay robustness. siRNA buffer (1×) (Horizon #B-002000-UB-
434 100) was aliquoted into wells, miRNA mimics were added so that the final concentration
435 was 40 nM/well, and DharmaFECT1/OptiMEM was dispensed into wells. While the
436 miRNA/lipid mix was allowed to complex, cells were trypsinized, counted, and
437 resuspended to reach a plating density of 600 cells/well. Cells were seeded on top of the
438 miRNA/lipid mixture, briefly centrifuged, and incubated for 72 hours, a time that we
439 determined to be optimal for p53 stabilization for small miRNAs. The cells were then
440 equilibrated to room temperature (~15 min) before analysis. Using TTP LabTech's Acumen
441 eX3 laser scanning cytometer, the total EGFP and DsRed intensities in each well were
442 quantitated. Internal controls were present in Columns 13 and 14 of each library plate
443 (Pre-miR miRNA Precursor Molecules Negative Control #1 - Ambion AM17110; Pre-miR
444 miRNA Precursor Molecules Negative Control #2 – Ambion AM17111; PLK1 SMARTpool
445 Dharmacon M-003290-01). In addition, siRNAs against E6AP (UBE3A, Dharmacon D-
446 005137-04) and non-targeting siRNAs (Dharmacon D-001210-01 and D-001210-02) were

447 added to each plate. The miRNA mimics were screened in triplicate. High throughput
448 libraries and screening capability was provided by the ICCB-Longwood Screening Facility
449 at Harvard Medical School.

450 miRNA transfections

451 All cells were reverse transfected with miRNAs (Table 2) using RNAiMax according
452 to manufacturer's instructions (ThermoFisher Scientific). More specifically, 750 µl of
453 suspended cells were added to 250 µl of a transfection mix containing 2 µl of Lipofectamine
454 RNAiMax and different miRNAs for a final concentration of 10nM and plated in 12-well
455 plates. miRNA transfection efficiency in different cell lines was confirmed using siGlo Red
456 Transfection Indicator (Horizon, D-001630-02-05).

457 Confirmation assay

458 HeLa cells were reverse transfected with 10 nM of the indicated miRNAs using
459 Lipofectamine RNAiMAX according to manufacturer's instructions. 72h after transfection
460 the cells were trypsinized, harvested in 1X flow cytometry buffer (1X PBS, 1mM EDTA, 2%
461 FBS) and analyzed for green and red fluorescence by flow cytometry using a BD
462 FACSymphony instrument (BD-Biosciences).

463 Western blots and antibodies

464 After incubation for 72h, transfected cells were washed once with 1X PBS, lysed
465 directly in wells with 100-150µl of SDS Lysis buffer (62.5mM Tris-Cl, pH 6.8, 2% SDS) and
466 sonicated (amplitude of 35%; 10 pulses with 2 seconds ON and 0.5 seconds OFF). The
467 lysates were centrifuged for 2 minutes and protein concentrations quantitated by BCA
468 Protein Assay (Pierce). Lysates (10 µg of protein/well) were run on 20-well 4-12% NuPage

469 BisTris midi gels in 1X MES buffer (ThermoFisher Scientific) and transferred to
470 polyvinylidene difluoride (PVDF) membranes using 25 mM Tris-HCl pH 7.6, 192 mM
471 glycine, and 10% methanol. Membranes were blocked in 5% nonfat dried milk in Tris-
472 buffered saline [pH 7.4], 0.05% Tween 20 (TBST) and then incubated with primary
473 antibodies as follows: mouse monoclonal anti-E6AP (clone E4) at 1:1000 dilution (sc-
474 166689 from Santa Cruz Biotechnology); rabbit monoclonal anti-cleaved PARP (Asp214)
475 (D64E10 XP® #5625 from Cell Signaling Technologies); mouse monoclonal anti-HPV18-E6
476 (clone G-7) at a 1:250 dilution (sc-365089 from Santa Cruz Biotechnology); mouse
477 monoclonal anti-p21 Waf1/Cip1/CDKN1A (clone 187) at a 1:1000 dilution (sc-817 from
478 Santa Cruz Biotechnology); and mouse monoclonal anti-HPV18-E7 (clone F-7) at a 1:250
479 dilution (sc-365035 from Santa Cruz Biotechnology). Membranes were washed in TBST
480 and incubated with horseradish peroxidase (HRP)-conjugated anti-mouse antibody at a
481 1:1,000 dilution (R1005 from Kindle Biosciences). The primary antibodies against β-Actin
482 and P53 were directly conjugated to HRP and were used as follows: mouse monoclonal
483 anti-β-Actin-HRP at a 1:50,000 dilution (A3854 from Millipore Sigma); and goat polyclonal
484 anti-p53-HRP at a 1:3,000 dilution (HAF1355 from R&D systems). All blots were developed
485 using KwikQuant Ultra Digital-ECL™ Substrate Solution and processed using KwikQuant™
486 Imager (Kindle Bioscience LLC). Western blots were quantified using the Image Studio Lite
487 program (LI-COR Biotechnologies).

488 RNA isolation and qRT-PCR.

489 At 72h post-transfection, total RNA was isolated using the Nucleospin RNA kit
490 (Takara Bio) according to the manufacturer's instructions. Samples were quantified using
491 NanoDrop™ Lite Spectrophotometer and equal amounts of RNA (500ng) were reverse

492 transcribed using the high-capacity cDNA reverse transcription kit (Applied Biosystems).
493 Quantitative real-time PCR (qRT-PCR) was performed in an Applied Biosystems ABI 7500
494 fast sequence detection system using TaqMan Fast Advanced Master Mix (ThermoFisher
495 Scientific), and the following TaqMan custom gene expression assays for HPV18-E6E7:
496 HPV18-E6E7 FWD 5'-CAACCGAGCACGACAGGAA-3'; HPV18-E6E7 PROBE 5'-
497 AATATTAAGTATGCATGGACCTAAGGCAACATTGCAA-3'; and HPV18-E6E7 REV 5'-
498 CTCGTCGGGCTGGTAAATGTT-3' and for HPV16-E6E7: HPV16-E6-FWD 5'-
499 AGGAGCGACCCGGAAAGT-3'; HPV16-E6-PROBE 5'-
500 ACCACAGTTATGCACAGAGCTGCAAACAA-3'; and HPV16-E6-REV 5'-
501 CACGTCGCAGTAACTGTTGCTT-3'. All reactions were normalized using a TaqMan gene
502 expression assay for PPIA (Hs99999904_m1 ThermoFisher Scientific).

503 **Luciferase assays**

504 C33A cells were transfected in 12-well plates with 10 nM of miRNAs as described
505 above. After 24h, the miRNA transfection mix was removed and cells were transfected with
506 0.5 μg of either plasmid pGL4-LCRHPV16 (p6239, HPV16 nt 7000-85) (49) or pGL4-
507 LCRHPV18 (p5194, HPV18 nt 6943-105) (50), containing the firefly luciferase ORF under
508 the control of the HPV16 and HPV18 LCRs respectively, together with 0.5μg of a plasmid
509 expressing the renilla luciferase under the control of the human β-actin promoter using
510 Lipofectamine 3000 (ThermoFisher Scientific) according to manufacturer's protocol. At
511 48h post-transfection of plasmids (72 hours after miRNA transfection), cells were lysed in
512 the plate with 250 μl of 1x Passive Lysis Buffer and luciferase activity was determined
513 using the Dual-Luciferase Reporter Assay System (Promega) according to the
514 manufacturer's instructions. Luciferase intensities were measured using a SpectraMax L

515 luminescence microplate reader (Molecular Devices). Firefly luciferase readings were
516 normalized to the respective renilla luciferase readings.

517 Apoptosis assays

518 HeLa cells were reverse transfected with 10 nM of the different miRNAs either alone
519 or combined with 20 nM of siRNAs directed to p53 (Dharmacon, D-003329-26: 5'-
520 GCUUCGAGAUGUUCCGAGA-3') or its C911 version (sense, 5'-GCUUCGAGUACUUCCGAGA-
521 UU-3') using Lipofectamine RNAiMAX according to manufacturer's instructions. After
522 incubation for 72h, attached cells were trypsinized and combined with all non-adherent
523 cells in the supernatant and PBS washes. The cells were stained with Annexin V using the
524 Dead Cell Apoptosis Kit with Annexin V Alexa Fluor™ 488 & Propidium Iodide (PI)
525 (ThermoFisher Scientific #V13241 and #V13245). Stained cells were analyzed by flow
526 cytometry using a BD FACSCanto flow cytometer (BD Biosciences).

527 Figures and statistics

528 All graphics and statistical analyses were conducted using Prism 8 (GraphPad).
529 When the values corresponding to mock transfections were used to normalize other values
530 obtained in an experiment, the mock values were not included in the corresponding
531 graphic since invariably their mean is equal to one and their standard deviation is zero.
532 Figures were assembled using Affinity Photo (Affinity).
533

534 **Table 1. miRNAs selected from primary screen**

535

Rank	miRNA	Mature_Sequence	EGFP / DsRed (Mean, n = 3)	EGFP / DsRed (SD, n =3)
1	hsa-miR-375-3p	UUUGUUCGUUCGGCUCGCGUGA	0.12298	0.01761
2	hsa-miR-219a-5p	UGAUUGUCCAAACGCAAUUCU	0.07703	0.00559
3	hsa-miR-511-5p	GUGUCUUUUGCUCUGCAGUCA	0.07371	0.00962
4	hsa-miR-519c-3p	AAAGUGCAUCUUUUUAGAGGAU	0.07180	0.01690
5	hsa-miR-943	CUGACUGUUGCCGUCCUCCAG	0.06086	0.02073
6	hsa-miR-200c-5p	CGUCUUACCCAGCAGUGUUUGG	0.05781	0.00790
7	hsa-miR-944	AAAUUAUUGUACAUCGGAUGAG	0.05766	0.03304
8	hsa-miR-106a-3p	CUGCAAUGUAAGCACUUCUUAC	0.05210	0.00779
9	hsa-miR-374b-5p	AUAUAAUACAACCUGCUAAGUG	0.05065	0.00389
10	hsa-miR-148b-5p	AAGUUCUGUUAUACACUCAGGC	0.05013	0.00438
11	hsa-miR-519d-3p	CAAAGUGCCUCCCUUUAGAGUG	0.04929	0.01507
12	hsa-miR-631	AGACCUGGCCCAGACCUCAGC	0.04839	0.01369
13	hsa-miR-592	UUGUGUCAAUAUGCGAUGAUGU	0.04690	0.01220
14	hsa-miR-519b-3p	AAAGUGCAUCCUUUUAGAGGUU	0.04442	0.01903
15	hsa-miR-93-3p	ACUGCUGAGCUAGCACUUCCCG	0.04441	0.00884
16	hsa-miR-340-5p	UUAUAAAGCAAUGAGACUGAUU	0.04336	0.00383
17	hsa-miR-508-3p	UGAUUGUAGCCUUUUGGAGUAGA	0.04083	0.00853
18	hsa-miR-374a-3p	UUAUAAUACAACCUGAUAAGUG	0.03978	0.00887
19	hsa-miR-520d-3p	AAAGUGCUUCUCUUUGGUGGGU	0.03790	0.01428
20	hsa-miR-520c-3p	AAAGUGCUUCCUUUUAGAGGGU	0.03290	0.01176
21	hsa-miR-520b-3p	AAAGUGCUUCCUUUUAGAGGG	0.03226	0.01171
22	hsa-miR-153-3p	UUGCAUAGUCACAAAAGUGAUC	0.03096	0.00799
23	hsa-miR-17-5p	CAAAGUGCUUACAGUGCAGGUAG	0.02945	0.01485
24	hsa-miR-519a-3p	AAAGUGCAUCCUUUUAGAGUGU	0.02878	0.00725
25	hsa-miR-1287-5p	UGCUGGAUCAGUGGUUCGAGUC	0.02854	0.00375
26	hsa-miR-373-3p	GAAGUGCUUCGAUUUUGGGGUGU	0.02800	0.00787
27	hsa-miR-302a-3p	UAAGUGCUUCCAUGUUUUGGUGA	0.02791	0.00701
28	hsa-miR-302b-3p	UAAGUGCUUCCAUGUUUUAGUAG	0.02749	0.01175
29	hsa-miR-509-3p	UGAUUGGUACGUCUGUGGGUAG	0.02568	0.00559
30	hsa-miR-210-3p	CUGUGCGUGUGACAGCGGCUGA	0.02560	0.00996
31	hsa-miR-302c-3p	UAAGUGCUUCCAUGUUUCAGUGG	0.02376	0.00492
32	hsa-let-7a-2-3p	CUGUACAGCCUCCUAGCUUUCC	0.02275	0.01039
33	hsa-miR-224-5p	CAAGUCACUAGUGGUUCCGUU	0.02230	0.00997

536
537
538
539
540
541
542
543

544 **Table 2. miRNAs used in this study**

545

Description	Vendor	catalog number
miRIDIAN microRNA Human hsa-miR-375 - Mimic, 2 nmol	Dharmacon	C-300682-05-0002
miRIDIAN microRNA Human hsa-miR-219a-5p - Mimic, 2 nmol	Dharmacon	C-300576-05-0002
miRIDIAN microRNA Human hsa-miR-511-5p - Mimic, 2 nmol	Dharmacon	C-300752-03-0002
miRIDIAN microRNA Human hsa-miR-519c-3p - Mimic, 2 nmol	Dharmacon	C-300786-03-0002
miRIDIAN microRNA Human hsa-miR-943 - Mimic, 2 nmol	Dharmacon	C-301275-01-0002
miRIDIAN microRNA Human hsa-miR-200c-5p - Mimic, 2 nmol	Dharmacon	C-301070-01-0002
miRIDIAN microRNA Human hsa-miR-944 - Mimic, 2 nmol	Dharmacon	C-301276-01-0002
miRIDIAN microRNA Human hsa-miR-106a-3p - Mimic, 2 nmol	Dharmacon	C-301159-01-0002
miRIDIAN microRNA Human hsa-miR-374b-5p - Mimic, 2 nmol	Dharmacon	C-301250-01-0002
miRIDIAN microRNA Human hsa-miR-148b-5p - Mimic, 2 nmol	Dharmacon	C-301087-01-0002
miRIDIAN microRNA Human hsa-miR-519d-3p - Mimic, 2 nmol	Dharmacon	C-300812-05-0002
miRIDIAN microRNA Human hsa-miR-631 - Mimic, 2 nmol	Dharmacon	C-300957-01-0002
miRIDIAN microRNA Human hsa-miR-592 - Mimic, 2 nmol	Dharmacon	C-300916-01-0002
miRIDIAN microRNA Human hsa-miR-519b-3p - Mimic, 2 nmol	Dharmacon	C-300791-05-0002
miRIDIAN microRNA Human hsa-miR-93-3p - Mimic, 2 nmol	Dharmacon	C-301207-01-0002
miRIDIAN microRNA Human hsa-miR-340-5p - Mimic, 2 nmol	Dharmacon	C-301081-01-0002
miRIDIAN microRNA Human hsa-miR-508-3p - Mimic, 2 nmol	Dharmacon	C-300848-05-0002
miRIDIAN microRNA Human hsa-miR-374a-5p - Mimic, 2 nmol	Dharmacon	C-300681-05-0002
miRIDIAN microRNA Human hsa-miR-520d-3p - Mimic, 2 nmol	Dharmacon	C-300816-05-0002
miRIDIAN microRNA Human hsa-miR-520c-3p - Mimic, 2 nmol	Dharmacon	C-300803-05-0002
miRIDIAN microRNA Human hsa-miR-520b - Mimic, 2 nmol	Dharmacon	C-300797-03-0002
miRIDIAN microRNA Human hsa-miR-153-3p - Mimic, 2 nmol	Dharmacon	C-300615-07-0002
miRIDIAN microRNA Human hsa-miR-519a-3p - Mimic, 2 nmol	Dharmacon	C-300836-05-0002
miRIDIAN microRNA Human hsa-miR-1287-5p - Mimic, 2 nmol	Dharmacon	C-301341-00-0002
miRIDIAN microRNA Human hsa-miR-373-3p - Mimic, 2 nmol	Dharmacon	C-300680-03-0002
miRIDIAN microRNA Human hsa-miR-302a-3p - Mimic, 2 nmol	Dharmacon	C-300653-05-0002
miRIDIAN microRNA Human hsa-miR-302b-3p - Mimic, 2 nmol	Dharmacon	C-300669-05-0002
miRIDIAN microRNA Human hsa-miR-509-3p - Mimic, 2 nmol	Dharmacon	C-300849-07-0002
miRIDIAN microRNA Human hsa-miR-210-3p - Mimic, 2 nmol	Dharmacon	C-300565-03-0002
miRIDIAN microRNA Human hsa-miR-302c-3p - Mimic, 2 nmol	Dharmacon	C-300671-05-0002
miRIDIAN microRNA Human hsa-let-7a-2-3p - Mimic, 2 nmol	Dharmacon	C-301297-00-0002
miRIDIAN microRNA Human hsa-miR-224-5p - Mimic, 2 nmol	Dharmacon	C-300581-07-0002
miRIDIAN microRNA Human hsa-miR-302d-3p - Mimic, 2 nmol	Dharmacon	C-300672-05-0002
miRIDIAN microRNA Human hsa-miR-520e - Mimic, 2 nmol	Dharmacon	C-300772-03-0002
miRIDIAN microRNA Human hsa-miR-520a-3p - Mimic, 2 nmol	Dharmacon	C-300788-03-0002
miRIDIAN microRNA hsa-miR-20a-3p mimic, 2 nmol	Dharmacon	C-301022-01-0002
miRIDIAN microRNA Human hsa-miR-498 - Mimic, 2 nmol	Dharmacon	C-300771-03-0002
miRIDIAN microRNA Human hsa-miR-665 - Mimic, 2 nmol	Dharmacon	C-301246-01-0003
miRIDIAN microRNA Mimic Negative Control #1, 5 nmol	Dharmacon	CN-001000-01-05

546

547 # Acknowledgements

548 We thank other members of the Howley laboratory for helpful discussions and
549 suggestions. All plasmids generated in the Howley laboratory that are described in this
550 manuscript are available through Addgene. GMN, JAS and PMH are co-inventors on a patent
551 filed by Harvard on the therapeutic use of miRNAs in hrHPV positive cancers. This work
552 has been supported by NIH grant R35CA197262 to P.M.H.

553

554 # Bibliography

555 1. Schiller JT, Lowy DR. 2021. Papillomaviruses, p 45-67. *In* Knipe DM, Howley PM
556 (ed), Fields Virology, 7th ed, vol 2. Wolkers Kluwers, Philadelphia.
557 2. de Martel C, Plummer M, Vignat J, Franceschi S. 2017. Worldwide burden of cancer
558 attributable to HPV by site, country and HPV type. Int J Cancer 141:664-670.
559 3. Goodwin EC, DiMaio D. 2000. Repression of human papillomavirus oncogenes in
560 HeLa cervical carcinoma cells causes the orderly reactivation of dormant tumor
561 suppressor pathways. Proc Natl Acad Sci U S A 97:12513-8.
562 4. Wells SI, Francis DA, Karpova AY, Dowhanick JJ, Benson JD, Howley PM. 2000.
563 Papillomavirus E2 induces senescence in HPV positive cells via pRB- and $p21^{CIP}$-
564 dependent pathways. EMBO J 19:5762-5771.
565 5. Scheffner M, Werness BA, Huibregtse JM, Levine AJ, Howley PM. 1990. The E6
566 oncoprotein encoded by human papillomavirus types 16 and 18 promotes the
567 degradation of p53. Cell 63:1129-36.

568 6. Huibregtse JM, Scheffner M, Howley PM. 1993. Cloning and expression of the cDNA
569 for E6-AP: A protein that mediates the interaction of the human papillomavirus E6
570 oncoprotein with p53. Mol Cell Biol 13:775-784.
571 7. Huibregtse JM, Scheffner M, Howley PM. 1993. Localization of the E6-AP regions that
572 direct HPV E6 binding, association with p53, and ubiquination of associated
573 proteins. Mol Cell Biol 13:4918-4927.
574 8. Scheffner M, Huibregtse JM, Vierstra RD, Howley PM. 1993. The HPV-16 E6 and E6-
575 AP complex functions as a ubiquitin-protein ligase in the ubiquination of p53. Cell
576 75:495-505.
577 9. Park RB, Androphy EJ. 2002. Genetic analysis of high-risk e6 in episomal
578 maintenance of human papillomavirus genomes in primary human keratinocytes. J
579 Virol 76:11359-64.
580 10. Butz K, Ristriani T, Hengstermann A, Denk C, Scheffner M, Hoppe-Seyler F. 2003.
581 siRNA targeting of the viral E6 oncogene efficiently kills human papillomavirus-
582 positive cancer cells. Oncogene 22:5938-3945.
583 11. Chirayil R, Kincaid RP, Dahlke C, Kuny CV, Dalken N, Spohn M, Lawson B, Grundhoff
584 A, Sullivan CS. 2018. Identification of virus-encoded microRNAs in divergent
585 Papillomaviruses. PLoS Pathog 14:e1007156.
586 12. Wald AI, Hoskins EE, Wells SI, Ferris RL, Khan SA. 2011. Alteration of microRNA
587 profiles in squamous cell carcinoma of the head and neck cell lines by human
588 papillomavirus. Head Neck 33:504-12.

589 13. Wang X, Wang HK, Li Y, Hafner M, Banerjee NS, Tang S, Briskin D, Meyers C, Chow
590 LT, Xie X, Tuschl T, Zheng ZM. 2014. microRNAs are biomarkers of oncogenic human
591 papillomavirus infections. Proc Natl Acad Sci U S A 111:4262-7.
592 14. Tornesello ML, Faraonio R, Buonaguro L, Annunziata C, Starita N, Cerasuolo A,
593 Pezzuto F, Tornesello AL, Buonaguro FM. 2020. The Role of microRNAs, Long Non-
594 coding RNAs, and Circular RNAs in Cervical Cancer. Front Oncol 10:150.
595 15. Yen HC, Elledge SJ. 2008. Identification of SCF ubiquitin ligase substrates by global
596 protein stability profiling. Science 322:923-9.
597 16. Yen HC, Xu Q, Chou DM, Zhao Z, Elledge SJ. 2008. Global protein stability profiling in
598 mammalian cells. Science 322:918-23.
599 17. Hubbert NL, Sedman SA, Schiller JT. 1992. Human papillomavirus type 16 E6
600 increases the degradation rate of p53 in human keratinocytes. Journal of virology
601 66:6237-6241.
602 18. Scheffner M, Takahashi T, Huibregtse JM, Minna JD, Howley PM. 1992. Interaction of
603 the human papillomavirus type 16 E6 oncoprotein with wild-type and mutant
604 human p53 proteins. J Virol 66:5100-5.
605 19. Kamaraj B, Bogaerts A. 2015. Structure and Function of p53-DNA Complexes with
606 Inactivation and Rescue Mutations: A Molecular Dynamics Simulation Study. PLoS
607 One 10:e0134638.
608 20. Olotu FA, Soliman MES. 2019. Dynamic perspectives into the mechanisms of
609 mutation-induced p53-DNA binding loss and inactivation using active perturbation
610 theory: Structural and molecular insights toward the design of potent reactivators in
611 cancer therapy. J Cell Biochem 120:951-966.

612 21. Tomita Y, Marchenko N, Erster S, Nemajerova A, Dehner A, Klein C, Pan H, Kessler H,
613 Pancoska P, Moll UM. 2006. WT p53, but not tumor-derived mutants, bind to Bcl2
614 via the DNA binding domain and induce mitochondrial permeabilization. J Biol
615 Chem 281:8600-6.
616 22. Gencel-Augusto J, Lozano G. 2020. p53 tetramerization: at the center of the
617 dominant-negative effect of mutant p53. Genes Dev 34:1128-1146.
618 23. Jung HM, Phillips BL, Chan EK. 2014. miR-375 activates p21 and suppresses
619 telomerase activity by coordinately regulating HPV E6/E7, E6AP, CIP2A, and 14-3-
620 3zeta. Mol Cancer 13:80.
621 24. Martinez-Noel G, Vieira VC, Szajner P, Lilienthal EM, Kramer RE, Boyland KA, Smith
622 JA, Howley PM. 2021. Live cell, image-based high-throughput screen to quantitate
623 p53 stabilization and viability in human papillomavirus positive cancer cells.
624 Virology 560:96-109.
625 25. Munger K, Phelps WC, Bubb V, Howley PM, Schlegel R. 1989. The E6 and E7 genes of
626 the human papillomavirus type 16 together are necessary and sufficient for
627 transformation of primary human keratinocytes. J Virol 63:4417-21.
628 26. Liu X. 2018. Up-regulation of miR-20a by HPV16 E6 exerts growth-promoting effects
629 by targeting PDCD6 in cervical carcinoma cells. Biomed Pharmacother 102:996-
630 1002.
631 27. Scheffner M, Munger K, Byrne JC, Howley PM. 1991. The state of the p53 and
632 retinoblastoma genes in human cervical carcinoma cell lines. Proc Natl Acad Sci U S
633 A 88:5523-7.

634 28. Abdelmohsen K, Srikantan S, Tominaga K, Kang MJ, Yaniv Y, Martindale JL, Yang X,
635 Park SS, Becker KG, Subramanian M, Maudsley S, Lal A, Gorospe M. 2012. Growth
636 inhibition by miR-519 via multiple p21-inducing pathways. Mol Cell Biol 32:2530-
637 48.
638 29. Buehler E, Chen YC, Martin S. 2012. C911: A bench-level control for sequence
639 specific siRNA off-target effects. PLoS One 7:e51942.
640 30. Jiang Y, Hou R, Li S, Li S, Dang G. 2018. MicroRNA-302 inhibits cell migration and
641 invasion in cervical cancer by targeting DCUN1D1. Exp Ther Med 16:1000-1008.
642 31. Li GC, Cao XY, Li YN, Qiu YY, Li YN, Liu XJ, Sun XX. 2018. MicroRNA-374b inhibits
643 cervical cancer cell proliferation and induces apoptosis through the p38/ERK
644 signaling pathway by binding to JAM-2. J Cell Physiol 233:7379-7390.
645 32. Mou Z, Xu X, Dong M, Xu J. 2016. MicroRNA-148b Acts as a Tumor Suppressor in
646 Cervical Cancer by Inducing G1/S-Phase Cell Cycle Arrest and Apoptosis in a
647 Caspase-3-Dependent Manner. Med Sci Monit 22:2809-15.
648 33. Ji F, Du R, Chen T, Zhang M, Zhu Y, Luo X, Ding Y. 2020. Circular RNA circSLC26A4
649 Accelerates Cervical Cancer Progression via miR-1287-5p/HOXA7 Axis. Mol Ther
650 Nucleic Acids 19:413-420.
651 34. Abdelmohsen K, Kim MM, Srikantan S, Mercken EM, Brennan SE, Wilson GM, Cabo R,
652 Gorospe M. 2010. miR-519 suppresses tumor growth by reducing HuR levels. Cell
653 Cycle 9:1354-9.
654 35. Cai N, Wang YD, Zheng PS. 2013. The microRNA-302-367 cluster suppresses the
655 proliferation of cervical carcinoma cells through the novel target AKT1. Rna 19:85-
656 95.

657 36. Chen Y, Wang X. 2020. miRDB: an online database for prediction of functional
658 microRNA targets. Nucleic Acids Res 48:D127-D131.
659 37. Liu W, Wang X. 2019. Prediction of functional microRNA targets by integrative
660 modeling of microRNA binding and target expression data. Genome Biol 20:18.
661 38. Kuhnle S, Martinez-Noel G, Leclere F, Hayes SD, Harper JW, Howley PM. 2018.
662 Angelman syndrome-associated point mutations in the Zn(2+)-binding N-terminal
663 (AZUL) domain of UBE3A ubiquitin ligase inhibit binding to the proteasome. J Biol
664 Chem 293:18387-18399.
665 39. Kracikova M, Akiri G, George A, Sachidanandam R, Aaronson SA. 2013. A threshold
666 mechanism mediates p53 cell fate decision between growth arrest and apoptosis.
667 Cell Death Differ 20:576-88.
668 40. Bartel DP. 2009. MicroRNAs: target recognition and regulatory functions. Cell
669 136:215-33.
670 41. Shukla GC, Singh J, Barik S. 2011. MicroRNAs: Processing, Maturation, Target
671 Recognition and Regulatory Functions. Mol Cell Pharmacol 3:83-92.
672 42. Lee RC, Feinbaum RL, Ambros V. 1993. The C. elegans heterochronic gene lin-4
673 encodes small RNAs with antisense complementarity to lin-14. Cell 75:843-54.
674 43. Wightman B, Ha I, Ruvkun G. 1993. Posttranscriptional regulation of the
675 heterochronic gene lin-14 by lin-4 mediates temporal pattern formation in C.
676 elegans. Cell 75:855-62.
677 44. Bonneau E, Neveu B, Kostantin E, Tsongalis GJ, De Guire V. 2019. How close are
678 miRNAs from clinical practice? A perspective on the diagnostic and therapeutic
679 market. Ejifcc 30:114-127.

680 45. Hanna J, Hossain GS, Kocerha J. 2019. The Potential for microRNA Therapeutics and
681 Clinical Research. Front Genet 10:478.
682 46. Emanuele MJ, Elia AE, Xu Q, Thoma CR, Izhar L, Leng Y, Guo A, Chen YN, Rush J, Hsu
683 PW, Yen HC, Elledge SJ. 2011. Global identification of modular cullin-RING ligase
684 substrates. Cell 147:459-74.
685 47. Lin HC, Yeh CW, Chen YF, Lee TT, Hsieh PY, Rusnac DV, Lin SY, Elledge SJ, Zheng N,
686 Yen HS. 2018. C-Terminal End-Directed Protein Elimination by CRL2 Ubiquitin
687 Ligases. Mol Cell 70:602-613 e3.
688 48. Zhang JH, Chung TD, Oldenburg KR. 1999. A Simple Statistical Parameter for Use in
689 Evaluation and Validation of High Throughput Screening Assays. J Biomol Screen
690 4:67-73.
691 49. Ottinger M, Smith JA, Schweiger MR, Robbins D, Powell ML, You J, Howley PM. 2009.
692 Cell-type specific transcriptional activities among different papillomavirus long
693 control regions and their regulation by E2. Virology 395:161-71.
694 50. Schweiger MR, Ottinger M, You J, Howley PM. 2007. Brd4-independent
695 transcriptional repression function of the papillomavirus e2 proteins. J Virol
696 81:9612-22.

697

698 # Figure captions

699

700 **Figure 1. Primary screen.**

701 **A.** Reporter cassette of pHAGE-P CMVt RIG2 p53(R273C). The expressed open reading
702 frames are shown with the red and green arrows. CMVp: CMV promoter, IRES:
703 Encephalomyocarditis virus internal ribosomal entry site**. B.** Dot plot showing the effect of
704 the different miRNAs on individual experimental wells during the primary screen. Bars
705 indicate the means of triplicate experiments and the error bars show one standard
706 deviation. The split Y axis has two different scales to help with the visualization of the data.
707

708 **Figure 2. p53 stabilization in HeLa cells expressing the reporter pHAGE-P CMVt RIG3**
709 **p53(R273C).**

710 **A.** Reporter cassette in pHAGE-P CMVt RIG3 p53(R273C) (24). The expressed fusion
711 proteins are indicated with the red and green arrows. CMVp: CMV promoter, IRES:
712 Encephalomyocarditis virus internal ribosomal entry site, H2B: histone 2B (H2BC11), SG
713 linker: serine-glycine linker. **B.** 72 h after transfection cells were harvested and the
714 percentage of cells expressing mRuby-p53(R273C) was determined by flow cytometry.
715 Columns indicate the means of three independent experiments and the error bars show
716 one standard deviation. Variability between the means was tested using the one-way
717 ANOVA test ($F(40, 82) = 84.19$ $p<0.0001$). Then, each sample was compared to non-treated
718 cells using the "Dunnett's multiple comparisons test" (* = $p<0.01$).
719

720 **Figure 3. Effect of miRNAs transfection on p53, E6AP, and E6 protein levels in HeLa**
721 **cells.**

722 Cells were lysed 72 h post-transfection and the lysates were resolved by SDS-PAGE. Protein
723 levels of p53, E6AP, E6, and actin were visualized by western blotting. **A, C, and E.** Western

724 blot results from a single experiment. **B, D, and F.** Quantification of p53 from western blot
725 experiments. Values obtained for p53 were normalized to the amount of actin in the same
726 sample and then all values were divided by the corresponding value obtained with the
727 mock transfection in the same blot. Circles represent values from independent experiments
728 and the bars show the mean ± standard deviation. To determine significant differences
729 between the samples in an experiment we used the "one-way ANOVA" test (A. $F(16, 34)=8.271$ $p<0.0001$, $n=3$; B. $F(14, 30)=17.76$ $p<0.0001$, $n=3$; C. $F(3, 12)=52.63$ $p<0.0001$,
730
731 $n=4$). We then compared each sample with the cells transfected with the Ctrl.1 miRNA
732 using the "Dunnett's multiple comparisons test" (* = $p<0.01$).
733
734 **Figure 4. Quantification of the effect of miRNAs transfection on E6AP and E6 protein**
735 **levels in HeLa cells.**
736 Quantification of E6AP (**A-C**) and E6 (**D-F**) protein levels from western blot experiments.
737 The values for E6AP and E6 were normalized to the amount of actin in the same sample,
738 then all values were divided by the corresponding value of the mock transfection in the
739 same blot. Circles show the values of independent experiments and the bars indicate the
740 mean ± standard deviation. The significance of differences between the samples means
741 was determined using the one-way ANOVA test (A. E6AP protein levels $F(16, 34)=9.540$
742 $p<0.0001$, $n=3$; B. E6AP protein levels $F(14, 30)=1.218$ $p<0.3135$, $n=3$; C. E6AP protein
743 levels $F(3, 12)=11.16$ $p<0.0009$, $n=4$ D. E6 protein levels $F(16, 34)=8.672$ $p<0.0001$, $n=3$; E.
744 E6 protein levels $F(14, 30)=18.15$ $p<0.0001$, $n=3$; F. E6 protein levels $F(3, 12)=55.35$
745 $p<0.0001$, $n=4$). Each sample was then compared to the cells transfected with the Ctrl.1
746 miRNA using the "Dunnett's multiple comparisons test" (* = $p<0.01$). **G.** The protein levels

747 of p53, and E6 calculated from the western blot experiments were used to analyze whether
748 there is a significant correlation between the levels of these proteins after transfection of
749 HeLa cells with the different miRNAs. This was done by calculating the Pearson's
750 correlation coefficient (r) and a two tailed p value. **H.** Heat map summarizing the effect of
751 the miRNAs on the protein levels of E6, E6AP, and p53 relative to the cells transfected with
752 Ctrl.1 in the corresponding gel after averaging the quantifications of the western blot
753 experiments showed in Figures 3 and 4, and Table S2).
754
755 **Figure 5. Alignment of members of the 302/519 family of miRNAs.**
756 Several of the miRNAs identified in our screen have the same seed sequence indicated with
757 bold letters and underlined. The sequences of the miRNAs were aligned based on the most
758 common seed sequence found in this family framed with a dashed blue line. miRNAs of this
759 family present between the 32 miRNAs selected from the primary screen are indicated
760 with black letters.
761
762 **Figure 6. Effect of transfection of selected miRNAs on p53 and E6AP protein levels in**
763 **different cell lines.**
764 72 h after transfection cells were lysed and the protein extracts were resolved by SDS-
765 PAGE, and the p53, E6AP, and actin proteins levels were determined by western blotting.
766
767 **Figure 7. Effect of selected miRNAs on HPV E6 and E7 expression.**
768 Cells were harvested 72 h post-transfection and then used for the following experiments. **A.**
769 Western blot showing the effect of the selected miRNAs on E6, E7, and actin protein levels

770 in HeLa cells. **B.** Expression of the E6/E7 mRNAs after transfection of the selected miRNAs
771 was quantitated by QRT-PCR. Measures from each experiment were normalized to the
772 value of the corresponding mock transfection. Differences between samples were analyzed
773 by the "one-way ANOVA" test (HeLa $F(12, 39) = 42.32$ $p<0.0001$, n=4; SiHa $F(12, 26) =$
774 41.38 $p<0.0001$, n=3) , then each sample was compared to the corresponding non-treated
775 cells using the "Dunnett's multiple comparisons test" (* = $p<0.01$). **C.** Western blot showing
776 the effect of transfecting the indicated miRNAs into 1321 cells on the p53, E6AP, and actin
777 proteins levels after 72 h incubation. **D.** Effect of transfection of selected miRNAs on the
778 promoter activity of the HPV16 and HPV18 LCRs using a luciferase reporter assay in C33A
779 cells. Values from each experiment were normalized to the value obtained for the
780 corresponding mock transfection. Differences between samples were analyzed by the "one-
781 way ANOVA" test (HPV 16 LCR, $F(12, 38) = 34.91$ $p<0.0001$, n=4; HPV 18 LCR, $F(12, 39) =$
782 23.47 $p<0.0001$, n=4), then each sample was compared to the corresponding non-treated
783 cells using the "Dunnett's multiple comparisons test" (* = $p<0.01$). In B and D, circles
784 represent values from independent experiments and the bars show the mean ± standard
785 deviation.
786
787 **Figure 8. Transfection of selected miRNAs induces apoptosis in HeLa cells.**
788 **A.** Cells were harvested 72 h post-transfection and stained with Annexin V as an indicator
789 of apoptosis. The percentage of cells stained with Annexin V was determined by flow
790 cytometry. Variability between samples was first analyzed with the one-way ANOVA test
791 ($F(12,26)=48.04$ $p<0.0001$, n=3). Then each sample was compared to the non-treated cells
792 with the "Dunnett's multiple comparisons test" (* = $p<0.01$). Circles represent values from

793 independent experiments and the bars show the mean ± standard deviation. **B.** Cells were
794 transfected with the indicated miRNAs and 72 h later the cells were harvested and stained
795 with Annexin V as a marker for apoptosis. The percentage of Annexin V positive cells was
796 quantitated by flow cytometry. Variability between samples for each cell line was analyzed
797 with the one-way ANOVA test (SiHa $F(6,21)=45.17$ $p<0.0001$, n=4; C33A $F(6,21)=85.96$
798 $p<0.0001$, n=3; U2OS $F(6,21)=104.07$ $p<0.0001$, n=4). Each sample was then compared to
799 the non-treated cells with the "Dunnett's multiple comparisons test" (* = $p<0.01$). Circles
800 represent values from independent experiments and the bars show the mean ± standard
801 deviation. **C.** Effect of the indicated miRNAs on the p21 and actin proteins levels HeLa and
802 SiHa cells visualized by western blotting 72 h post transfection.
803
804 **Figure 9. p53 dependence of apoptotic effect of selected miRNAs in HeLa cells.**
805 **A.** Cells were transfected with the indicated miRNAs either alone or together with a siRNA
806 against p53 or its C911 variant. After incubation for 72 h the cells were harvested and
807 stained with Annexin V as a marker for apoptosis. The percentage of Annexin V stained
808 cells was determined by flow cytometry. The values obtained for the three transfections
809 with each miRNA were first analyzed with the one-way ANOVA test (375-3p $F(2, 6) = 3.075$
810 $p=0.1204$; 498-5p $F(2, 6) = 1.914$ $p=0.2276$; 20a-3p $F(2, 6) = 0.6553$ $p=0.5528$; 148b-5p
811 $F(2, 6) = 23.57$ $p=0.0014$; 374a-3p $F(2, 6) = 2.681$ $p=0.1472$; 519b-3p $F(2, 6) = 17.71$
812 $p=0.0030$; 1287-5p $F(2, 6) = 48.00$ $p=0.0002$). For all samples n=3. Then, the values from
813 samples transfected with the same miRNA were compared with each other using the
814 "Tukey's multiple comparisons test" (* = $p<0.01$). **B.** 72 h post-transfection cells were lysed

815 and the p53, cleaved PARP, and GAPDH proteins levels were determined by SDS-PAGE and

816 western blotting.

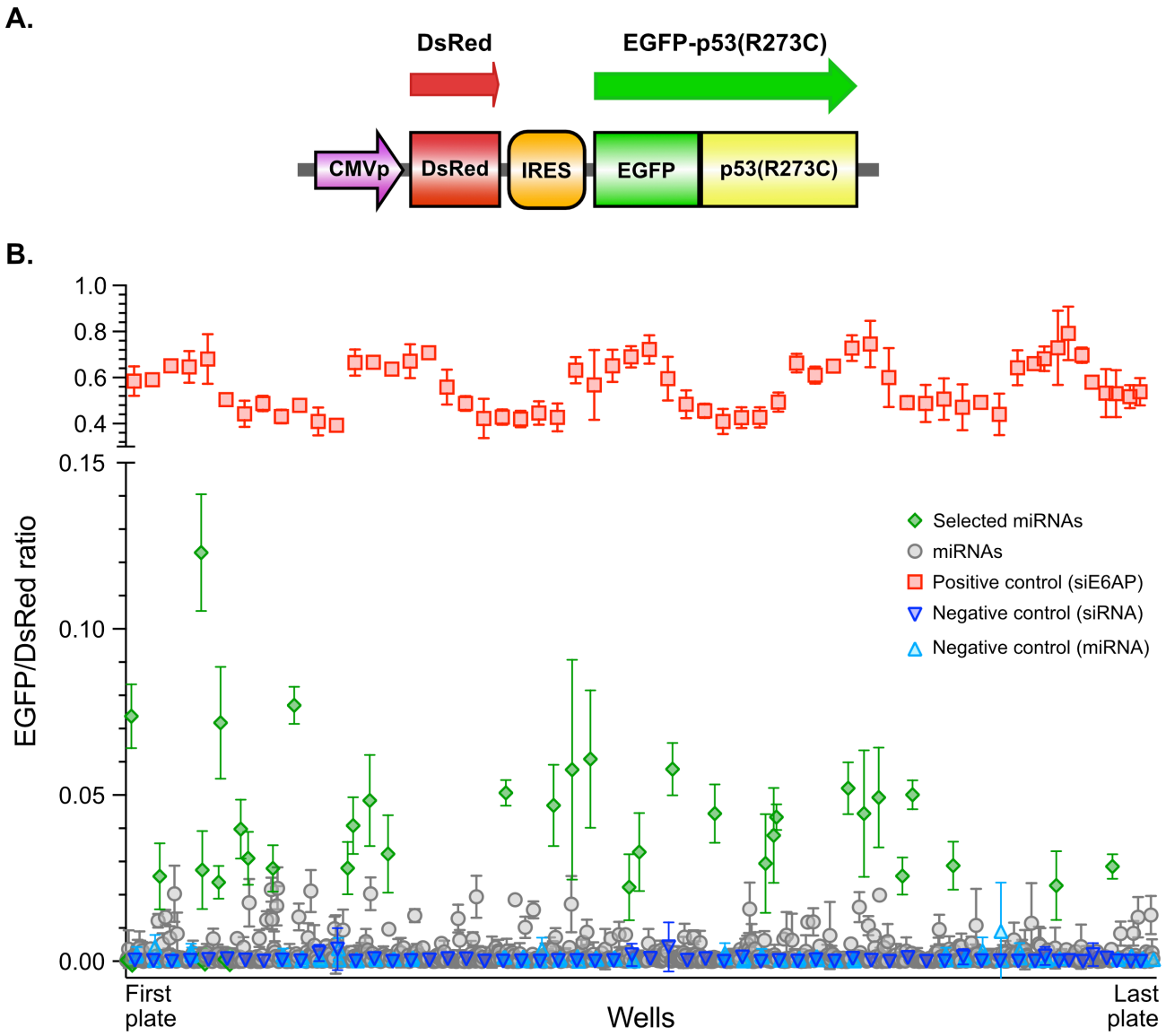
A.
DsRed
EGFP-p53(R273C)
CMVp
DsRed
IRES
EGFP
p53(R273C)
B.
1.0
0.8
0.6
0.4
0.15
0.10
0.05
0.00
EGFP/DsRed ratio
Selected miRNAs
miRNAs
Positive control (siE6AP)
Negative control (siRNA)
Negative control (miRNA)
First plate
Wells
Last plate

A.

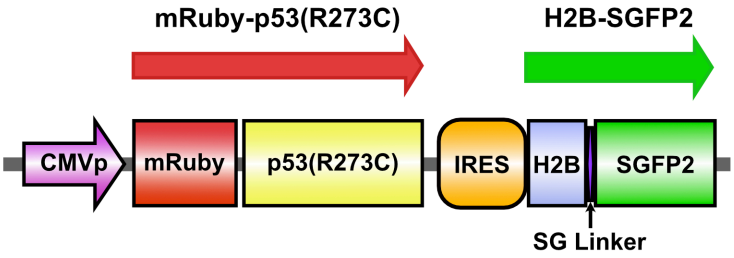
mRuby-p53(R273C)
H2B-SGFP2
CMVp
mRuby
p53(R273C)
IRES
H2B
SGFP2
SG Linker

B.

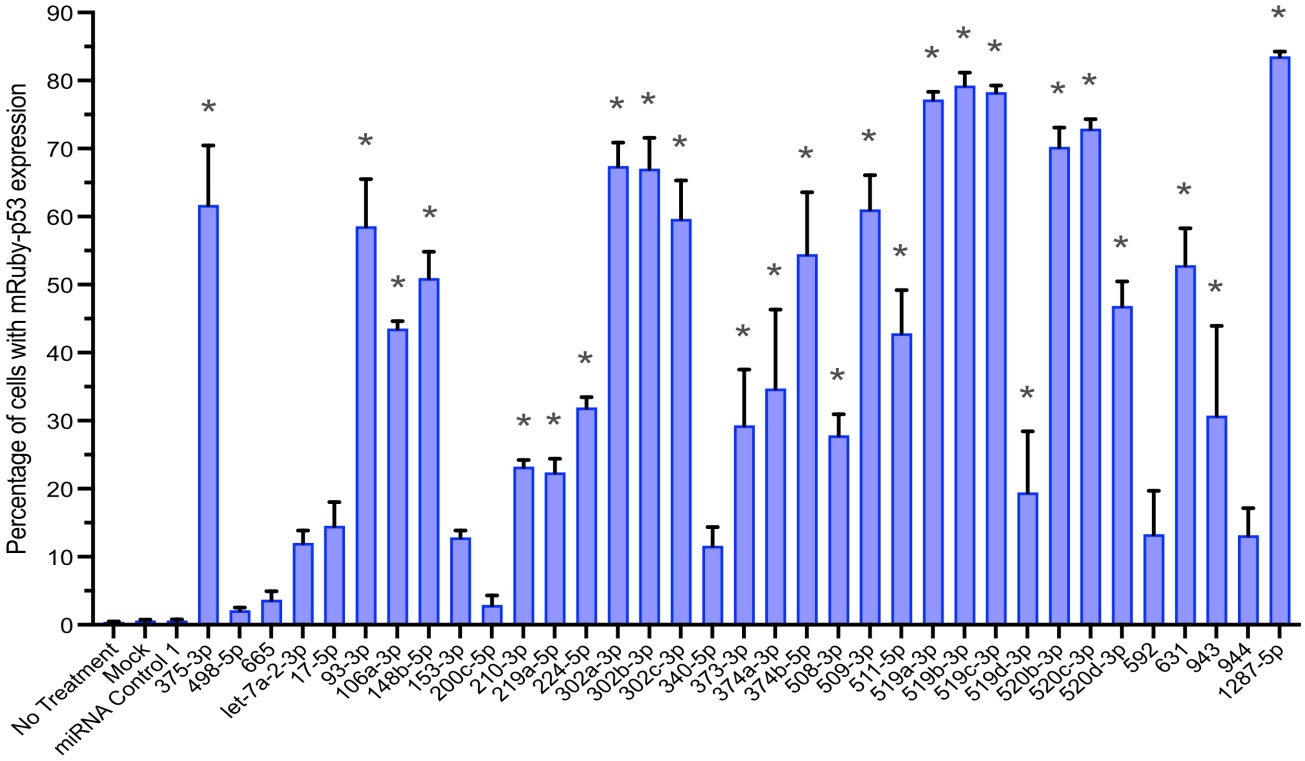
Percentage of cells with mRuby-p53 expression
0
10
20
30
40
50
60
70
80
90
No Treatment
Mock
miRNA Control 1
375-3p
498-5p
665
let-7a-2-3p
17-5p
93-3p
106a-3p
148b-5p
153-3p
200c-5p
210-3p
219a-5p
224-5p
302a-3p
302b-3p
302c-3p
340-5p
373-3p
374a-3p
374b-5p
508-3p
509-3p
511-5p
519a-3p
519b-3p
519c-3p
519d-3p
520b-3p
520c-3p
520d-3p
592
631
943
944
1287-5p

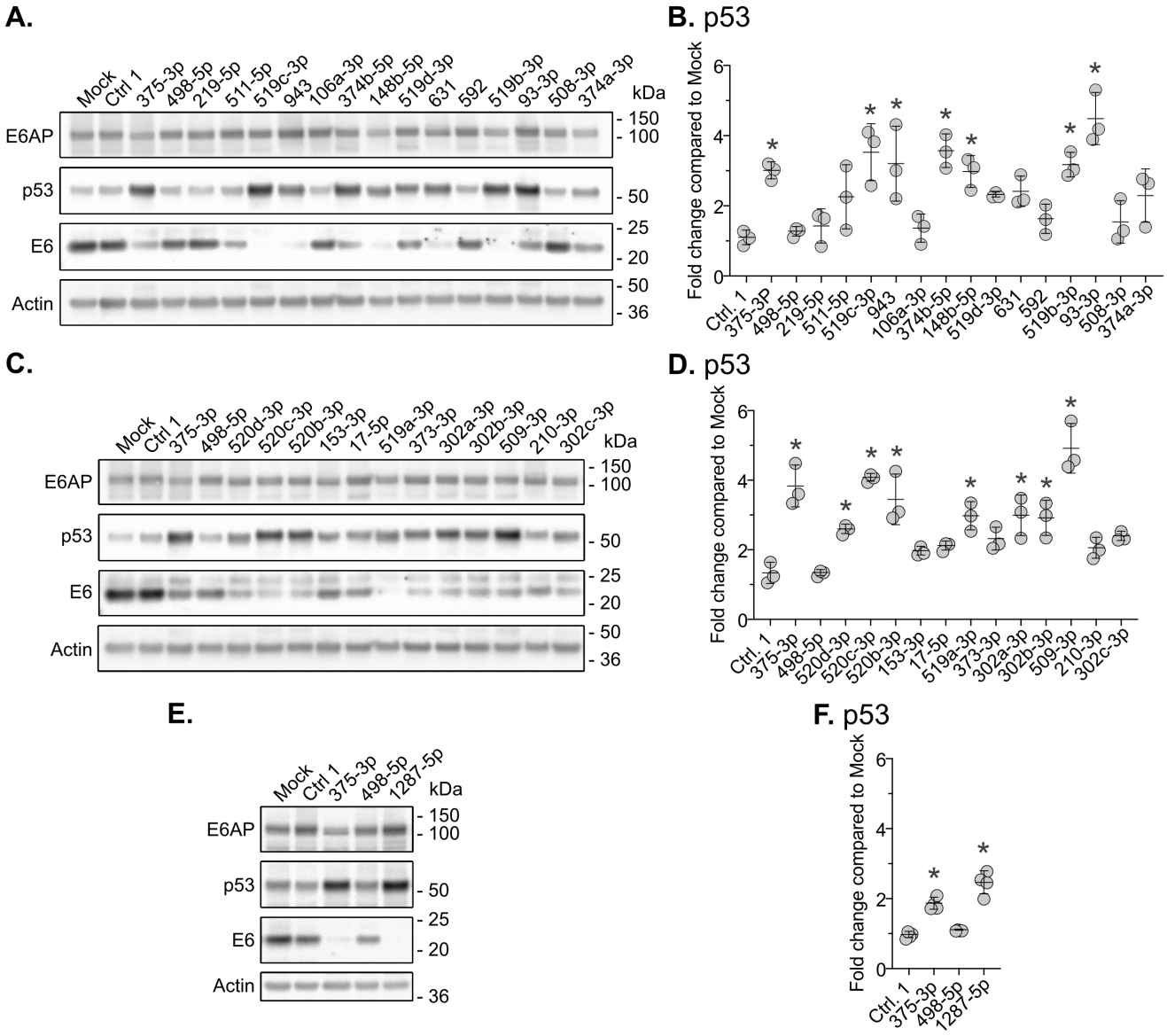
A.
Mock
Ctrl 1
375-3p
498-5p
219-5p
511-5p
519c-3p
943
106a-3p
374b-5p
148b-5p
519d-3p
631
592
519b-3p
93-3p
508-3p
374a-3p
kDa
E6AP
p53
E6
Actin
150
100
50
25
20
50
36
B. p53
Fold change compared to Mock
Ctrl. 1
375-3P
498-5p
219-5p
511-5p
519c-3p
943
106a-3p
374b-5p
148b-5p
519d-3p
631
592
519b-3p
93-3p
508-3p
374a-3p
C.
Mock
Ctrl 1
375-3p
498-5p
520d-3p
520c-3p
520b-3p
153-3p
17-5p
519a-3p
373-3p
302a-3p
302b-3p
509-3p
210-3p
302c-3p
kDa
E6AP
p53
E6
Actin
150
100
50
25
20
50
36
D. p53
Fold change compared to Mock
Ctrl. 1
375-3p
498-5p
520d-3p
520c-3p
520b-3p
153-3p
17-5p
519a-3p
373-3p
302a-3p
302b-3p
509-3p
210-3p
302c-3p
E.
Mock
Ctrl 1
375-3p
498-5p
1287-5p
kDa
E6AP
p53
E6
Actin
150
100
50
25
20
36
F. p53
Fold change compared to Mock
Ctrl. 1
375-3p
498-5p
1287-5p

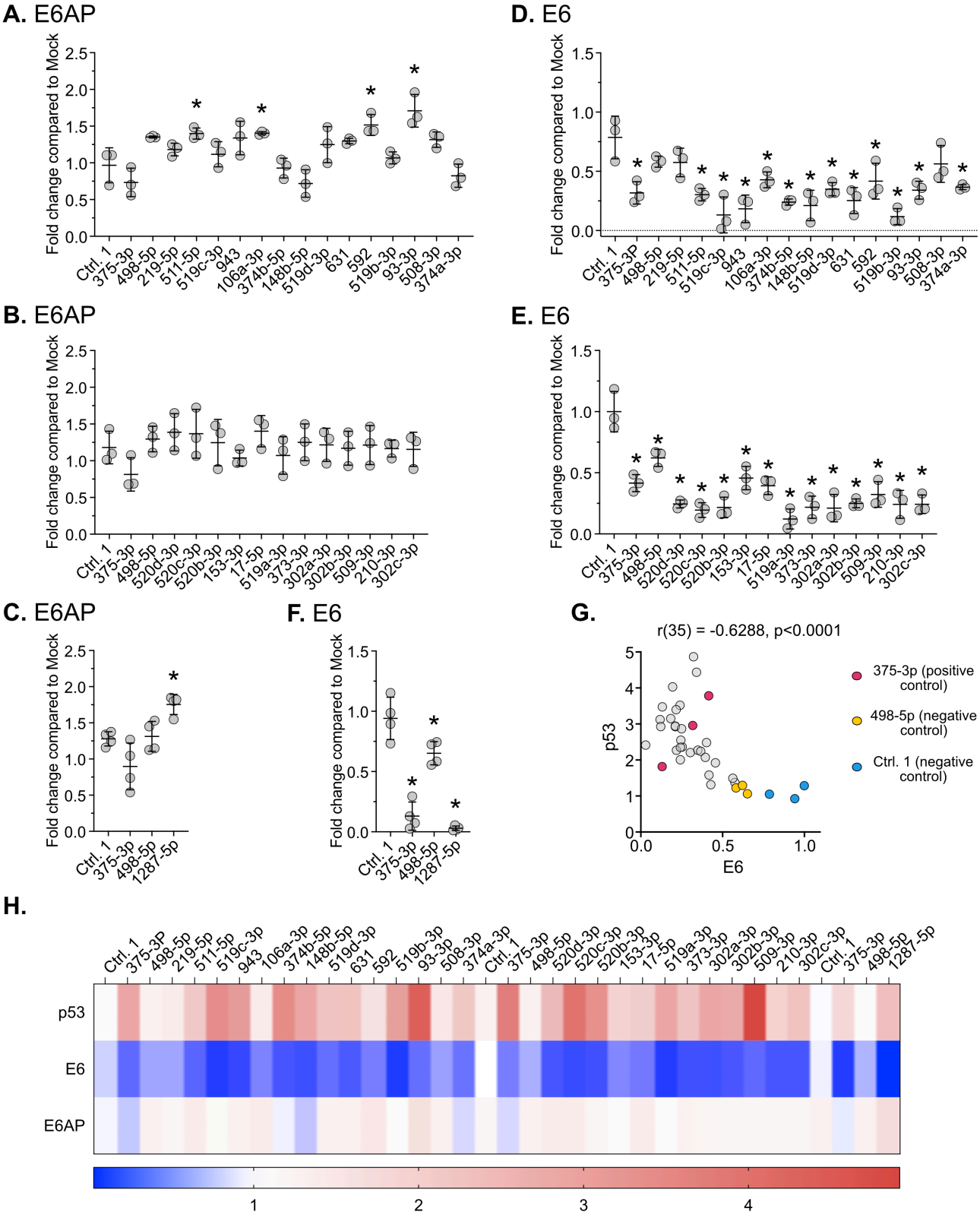
A. E6AP
Fold change compared to Mock
Ctrl. 1
375-3p
498-5p
219-5p
511-5p
519c-3p
943
106a-3p
374b-5p
148b-5p
519d-3p
631
592
519b-3p
93-3p
508-3p
374a-3p
D. E6
B. E6AP
520d-3p
520c-3p
520b-3p
153-3p
17-5p
519a-3p
373-3p
302a-3p
302b-3p
509-3p
210-3p
302c-3p
E. E6
C. E6AP
1287-5p
F. E6
G.
r(35) = -0.6288, p<0.0001
p53
E6
375-3p (positive control)
498-5p (negative control)
Ctrl. 1 (negative control)
H.
E6AP

302a-3p	U**AAGUGC**UUCCAUGUUUUGGUGA
302b-3p	U**AAGUGC**UUCCAUGUUUUAGUAG
302c-3p	U**AAGUGC**UUCCAUGUUUCAGUGG
302d-3p	U**AAGUGC**UUCCAUGUUUGAGUGU
372-3p	A**AAGUGC**UGCGACAUUUGAGCGU
373-3p	G**AAGUGC**UUCGAUUUUGGGGUGU
519a-3p	A**AAGUGC**AUCCUUUUAGAGUGU
519b-3p	A**AAGUGC**AUCCUUUUAGAGGUU
519c-3p	A**AAGUGC**AUCUUUUUAGAGGAU
519d-3p	C**AAAGUG**CCUCCCUUUAGAGUG
519e-3p	A**AGUGC**CUCCUUUUAGAGUGUU
520a-3p	A**AAGUGC**UUCCCUUUGGACUGU
520b-3p	A**AAGUGC**UUCCUUUUAGAGGG
520c-3p	A**AAGUGC**UUCCUUUUAGAGGGU
520d-3p	A**AAGUGC**UUCUCUUUGGUGGGU
520e-3p	A**AAGUGC**UUCCUUUUUGAGGG
520f-3p	A**AGUGCU**UCCUUUUAGAGGGUU
520g-3p	A**CAAAGU**GCUUCCCUUUAGAGUGU

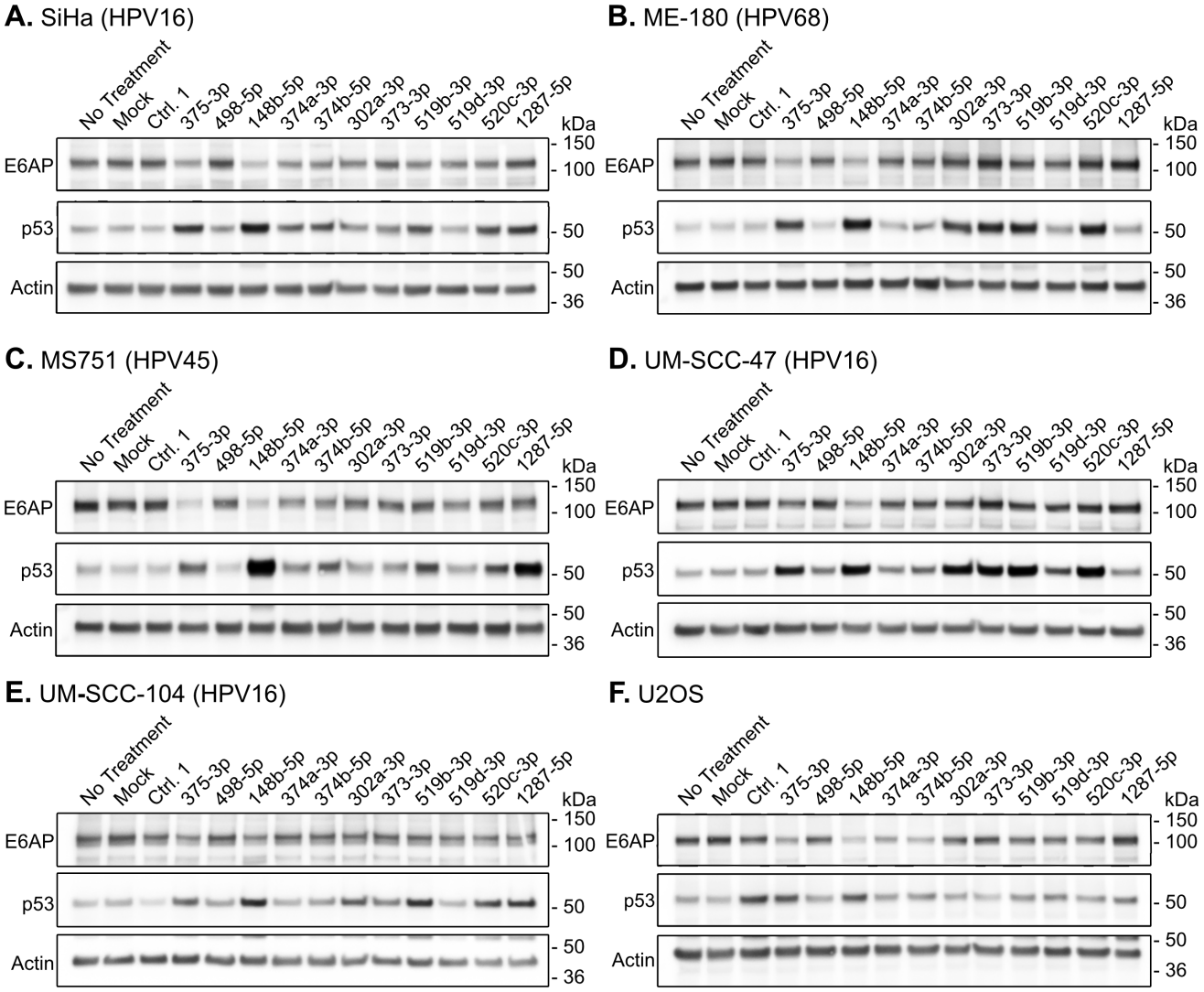
A. SiHa (HPV16)
B. ME-180 (HPV68)
C. MS751 (HPV45)
D. UM-SCC-47 (HPV16)
E. UM-SCC-104 (HPV16)
F. U2OS
No Treatment
Mock
Ctrl. 1
375-3p
498-5p
148b-5p
374a-3p
374b-5p
302a-3p
373-3p
519b-3p
519d-3p
520c-3p
1287-5p
kDa
E6AP
p53
Actin
150
100
50
50
36

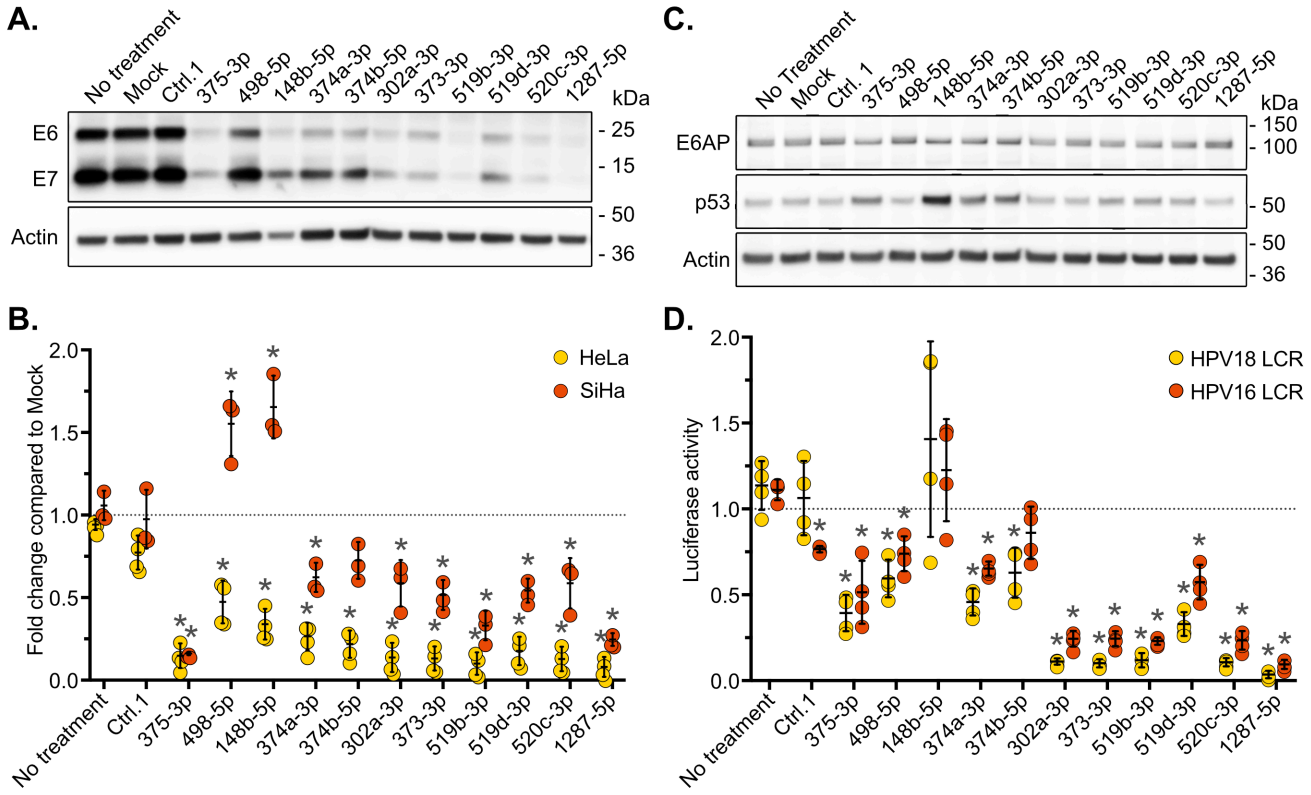
A.
No treatment
Mock
Ctrl.1
375-3p
498-5p
148b-5p
374a-3p
374b-5p
302a-3p
373-3p
519b-3p
519d-3p
520c-3p
1287-5p
kDa
E6
E7
Actin
- 25
- 15
- 50
- 36
B.
Fold change compared to Mock
HeLa
SiHa
C.
No Treatment
Mock
Ctrl. 1
375-3p
498-5p
148b-5p
374a-3p
374b-5p
302a-3p
373-3p
519b-3p
519d-3p
520c-3p
1287-5p
kDa
E6AP
p53
Actin
- 150
- 100
- 50
- 50
- 36
D.
Luciferase activity
HPV18 LCR
HPV16 LCR

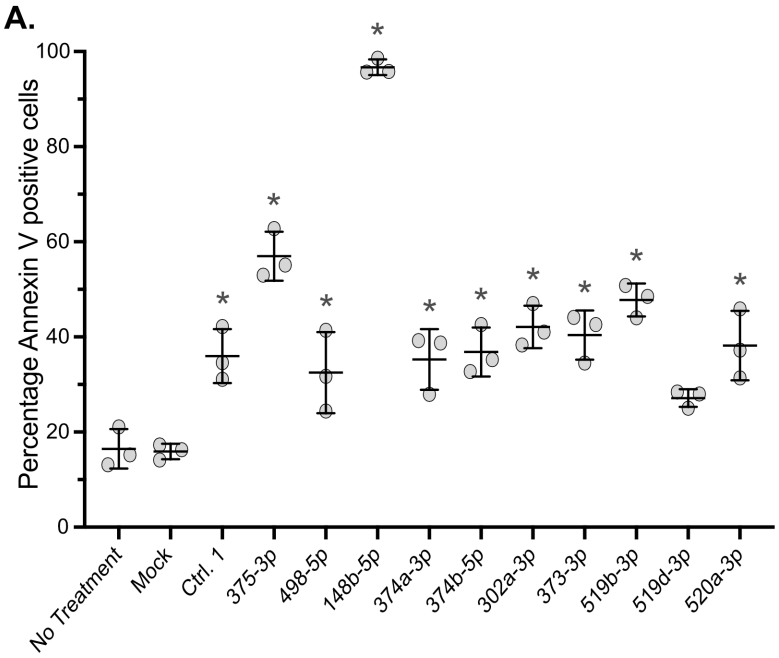
A.
Percentage Annexin V positive cells
100
80
60
40
20
0
No Treatment
Mock
Ctrl. 1
375-3p
498-5p
148b-5p
374a-3p
374b-5p
302a-3p
373-3p
519b-3p
519d-3p
520a-3p

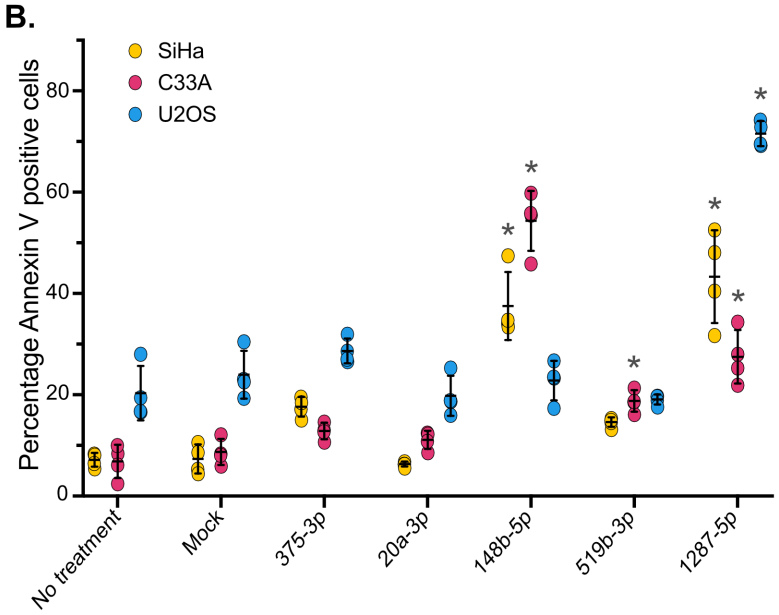
B.
SiHa
C33A
U2OS
Percentage Annexin V positive cells
80
60
40
20
0
No treatment
Mock
375-3p
20a-3p
148b-5p
519b-3p
1287-5p

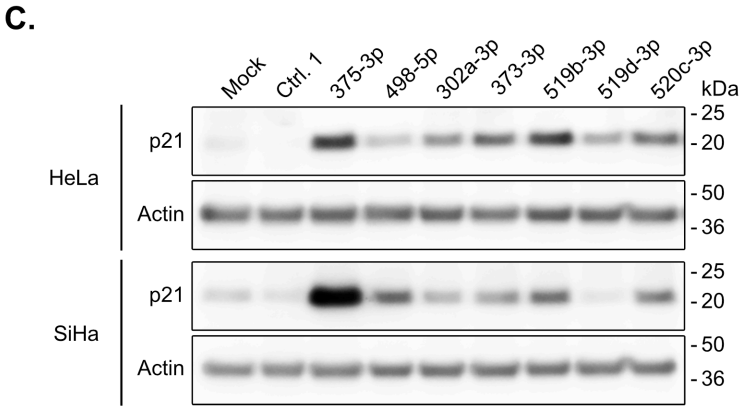
C.
Mock
Ctrl. 1
375-3p
498-5p
302a-3p
373-3p
519b-3p
519d-3p
520c-3p
kDa
HeLa
p21
Actin
SiHa
p21
Actin
25
20
50
36
25
20
50
36

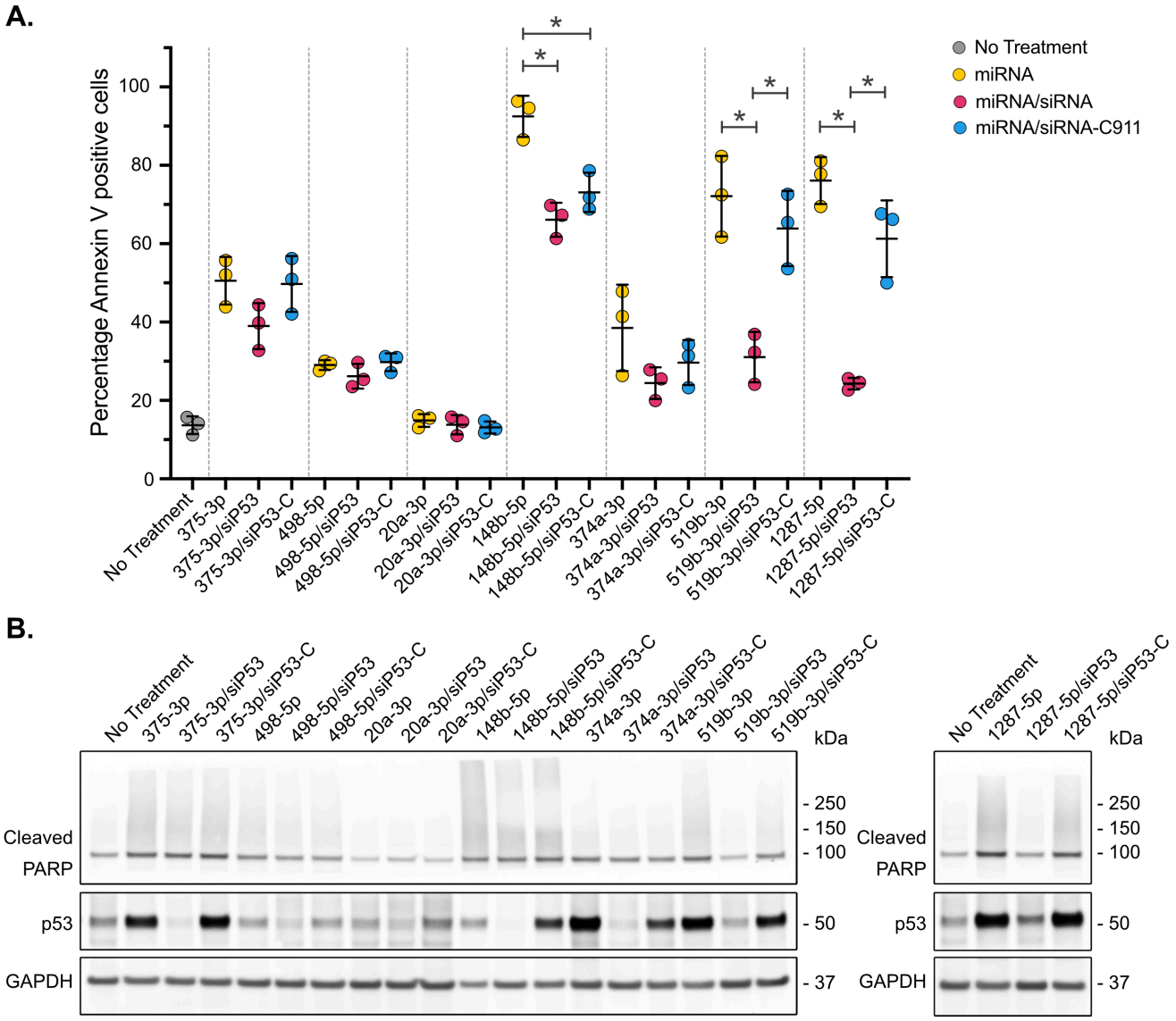
A.
Percentage Annexin V positive cells
0
20
40
60
80
100
No Treatment
miRNA
miRNA/siRNA
miRNA/siRNA-C911
No Treatment
375-3p
375-3p/siP53
375-3p/siP53-C
498-5p
498-5p/siP53
498-5p/siP53-C
20a-3p
20a-3p/siP53
20a-3p/siP53-C
148b-5p
148b-5p/siP53
148b-5p/siP53-C
374a-3p
374a-3p/siP53
374a-3p/siP53-C
519b-3p
519b-3p/siP53
519b-3p/siP53-C
1287-5p
1287-5p/siP53
1287-5p/siP53-C
B.
kDa
Cleaved PARP
p53
GAPDH
- 250
- 150
- 100
- 50
- 37
No Treatment
1287-5p
1287-5p/siP53
1287-5p/siP53-C